5-2022

Differential Transcriptome Analysis Reveals that Cache Valley PM2.5 Triggers the Unfolded Protein Response in Human Lung Cells

Morgan Eggleston
Utah State University

DIFFERENTIAL TRANSCRIPTOME ANALYSIS REVEALS THAT CACHE VALLEY $PM_{2.5}$ TRIGGERS THE UNFOLDED PROTEIN RESPONSE IN HUMAN LUNG CELLS

by

Morgan Eggleston

A thesis submitted in partial fulfillment

of the requirements for the degree

of

MASTER OF SCIENCE

in

Toxicology

Approved:

Roger A. Coulombe, Jr., Ph.D. Major Professor	Randal Martin, Ph.D. Committee Member
Kimberly Hageman, Ph.D. Committee Member	D. Richard Cutler, Ph.D. Interim Vice Provost for Graduate Studies

UTAH STATE UNIVERSTIY
Logan, Utah

2022

ABSTRACT

Differential Transcriptome Analysis Reveals that Cache Valley $PM_{2.5}$ Triggers the Unfolded Protein Response in Human Lung Cells

by

Morgan Eggleston, Master of Science

Utah State University, 2022

Major Professor: Dr. Roger A. Coulombe Jr.
Department: Animal Dairy and Veterinary Science

Fine ambient particulate matter ($PM_{2.5}$) poses a serious public health risk and is associated with increases in all-cause mortality, cardiopulmonary and cardiovascular disease, stroke, diabetes, cancer, and Alzheimer's disease. The normally picturesque Cache Valley of Northern Utah frequently experiences some of the highest $PM_{2.5}$ concentrations in the United States. However, the exact mechanism(s) of Cache Valley's $PM_{2.5}$ (CVPM) toxicity have yet to be fully characterized. We recently demonstrated that CVPM exposure is associated with the inflammatory response, endoplasmic reticulum (ER) stress, and the unfolded protein response (UPR), a highly conserved stress-response mechanism. The purpose of this study was to use whole transcriptome sequencing and network analysis to confirm the involvement of these mechanisms in cultured human lung (BEAS-2B) cells exposed to CVPM (1 and 12 μg/mL; 24 hr). All experiments were conducted in parallel with diesel exhaust particles (DEP) as a positive control. RNA sequencing with Ensemble Gene Set Enrichment Analysis (EGSEA) confirmed CVPM exposure significantly upregulated the UPR pathway (FDR adjusted p=0.05), specifically

altering the expression of PERK, IRE1, ATF-6, ATF-4, and CHOP genes. Significantly affected UPR-associated pathways included apoptosis, reactive oxygen species (ROS), and the inflammatory response. Flow cytometry revealed that CVPM exposure resulted in significant UPR-related cellular responses including reductions in mitochondrial membrane potential and alterations in intracellular Ca^{2+} homeostasis, as evidenced by a significant influx of Ca^{2+} in the cytosol and mitochondria, likely from the endoplasmic reticulum (ER). CVPM-associated late-stage apoptosis, increased ROS, and cytotoxicity were also observed. In most experiments, 1μg/mL DEP elicited similar results to 12μg/mL CVPM, suggesting that CVPM is less potent than DEP. Taken together, these results support our hypothesis that a principal toxic mechanism of CVPM pollution involves ER stress and the UPR. Identification of the UPR as an operative mechanism of $PM_{2.5}$ toxicity represents a significant enhancement of our understanding of air pollutant toxicology because activation of the UPR resulting from ER stress has been associated with the pathophysiology of many PM-related diseases, such as asthma, cardiovascular disease, neurodegenerative disease, and ischemic stroke.

(80 pages)

PUBLIC ABSTRACT

Differential Transcriptome Analysis Reveals that Cache Valley $PM_{2.5}$ Triggers the Unfolded Protein Response in Human Lung Cells

Morgan Eggleston

Worldwide, exposure to air pollution is a serious human health threat. Particulate matter (PM) air pollution is a mixture of suspended solid and/or liquid particles and particle size is determined by its aerodynamic diameter. Fine, or "respirable" particles, typically from vehicle emissions, manufacturing, power generation, agriculture, as well as secondary photochemical reactions, are classified as ≤2.5μm in diameter ($PM_{2.5}$). Upon inhalation, $PM_{2.5}$ particles can reach the lower, more sensitive regions of the lung, enter the bloodstream, and be distributed to other areas in the body. Large-scale epidemiology studies have shown that $PM_{2.5}$ air pollution is associated with increases in all-cause mortality, cardiopulmonary and cardiovascular disease, stroke, cancer, and Alzheimer's disease. The normally picturesque Cache Valley of Northern Utah frequently experiences some of the highest $PM_{2.5}$ concentrations in the United States during inversion events in the winter months. Elevated wintertime $PM_{2.5}$ concentrations in Cache Valley are primarily due to a combination of human activity and environmental factors. However, the exact mechanism(s) of Cache Valley $PM_{2.5}$ (CVPM) toxicity, or how CVPM may affect the health of Cache Valley residents, are not fully understood. Previous studies from our laboratory showed that CVPM exposure in cultured human lung cells is associated with the inflammatory response, endoplasmic reticulum (ER) stress, and the unfolded protein response (UPR), a well-known stress-response system in cells. The purpose of this study was to confirm our previous findings since our method

for collecting local CVPM was updated to a more effective particle collection system. In the present study, next-generation RNA sequencing revealed that human lung cells exposed to CVPM had gene expression changes related to activation of the UPR. Disruptions in normal cell conditions, or homeostasis, were also observed. Identification of the UPR as an operative mechanism of $PM_{2.5}$ toxicity will represent an important breakthrough in our understanding of pollutant toxicology because activation of the UPR has been linked to many serious diseases, such as diabetes, retinal degeneration, metabolic disease, and even cancer. My research is also significant because it will enable more accurate risk estimates of CVPM exposure and may help guide positive changes in government regulations to improve air quality.

ACKNOWLEDGMENTS

First and foremost, I would like to express my sincerest gratitude to Dr. Roger Coulombe for his continual guidance, mentorship, knowledge, and patience throughout every stage of my research project. I would like to extend my sincere thanks to my committee members, Dr. Randy Martin and Dr. Kimberly Hageman, for their support and invaluable insights, as well as the Marriner S. Eccles Foundation, the Center for Integrated Biosystems at Utah State University, and Cytiva. I would like to acknowledge my fellow students, Andy Nguyen and Nick Grooms, for their assistance on this project. I am also grateful to Dr. Mirella Meyer-Ficca for her insightful comments and suggestions. I also appreciate Cara Allen for her kindness and administrative help. Finally, I would like to thank my fiancé, Shane, for his tireless support and dedication to keeping us outdoors as much as possible.

CONTENTS

Page

LIST OF TABLES

Page

LIST OF FIGURES

Page

LIST OF ACRONYMS

Abbreviation	**Definition**
AD	Alzheimer's Disease
ADRM1	26S proteasomal ubiquitin receptor
AIP-1	Aryl hydrocarbon receptor interacting protein 1
Akt	Protein kinase β
ASK1/JNK	Apoptosis signal-regulating kinase 1/c-Jun N-terminal kinase
ATF-4	Activating transcription factor 4
ATF-6	Activating transcription factor 6
AQI	Air quality index
BAK	BCL2 antagonist/killer 1
BAX	BCL2-associated X apoptosis regulator
BEAS-2B	Human bronchial epithelial cell line
BI-1	BAX inhibitor 1
BiP	Binding immunoglobulin protein
Ca^{2+}	Calcium
CALR	Calreticulin
CAM	Calmodulin
CCCP	Carbonyl cyanide m-chlorophenyl hydrazone
CCK-8	Cell Counting Kit-8
CHOP	C/EBP homologous protein
CI	Confidence interval
COPD	Chronic obstructive pulmonary disease
CVPM	Cache Valley $PM_{2.5}$
CX3CL1	Fractalkine/chemokine (C-X3-C motif) ligand 1
DAQ	Division of Air Quality
DCFH-DA	2',7'-dichlorofluorescin diacetate
DE	Differential expression
DEG	Differentially expressed gene

DEP	Diesel exhaust particles
$DiOC_6$	3,3'-dihexyloxacarbocyanine iodide
EGSEA	Ensemble gene set enrichment analysis
eIF2α	Eukaryotic initiation factor 2 α
EPA	Environmental Protection Agency
ER	Endoplasmic reticulum
ERAD	Endoplasmic reticulum-associated protein degradation
FDR	False discovery rate
Fluo-3 AM	Fluo-3-pentaacetoxymethyl ester
GADD45B	Growth arrest and DNA damage inducible β
GCLM	Glutamate-cysteine ligase regulatory subunit
GPX4	Glutathione peroxidase 4
GRP94/HSP90B1	Glucose-regulated protein 94/Heat shock protein 90kDa
GSE	Gene set enrichment
GSR	Glutathione reductase
H_2O_2	Hydrogen peroxide
HNO_3	Nitric acid
HSPB1/Hsp27	Heat shock protein β-1/Heat shock protein 27
Hsp70	Heat shock protein 70kDa
IARC	International Agency for Research on Cancer
IFITM1	Interferon-induced transmembrane protein 1
IL-1	Interleukin 1
IL1A	Interleukin-1α
IL1B	Interleukin-1β
IL1-R1	Interleukin 1 receptor type 1
IL-6	Interleukin 6
IL-6R	Interleukin 6 receptor
IL-8	Interleukin 8
IL-18	Interleukin 18
IL-20	Interleukin 20

IP3R	Inositol triphosphate receptor
IRAK	Interleukin 1 receptor-associated kinase
IRAK2	Interleukin-1 receptor-associated kinase 2
IRE1	Inositol-requiring enzyme 1
logCPM	Log counts per million
logFC	Log-fold change
MAM	Mitochondrial associated membrane
Mcl-1	Myeloid-cell leukemia 1
MICA	MHC class I polypeptide-related sequence A
mRNA	Messenger RNA
MSigDB	Molecular Signatures Database
NAAQS	National Ambient Air Quality Standards
NF-κβ	Nuclear factor-κβ
NH_3	Ammonia
NH_4Cl	Ammonium chloride
NH_4NO_3	Ammonium nitrate
NO	Nitric oxide
NO_2	Nitrogen dioxide
O_3	Ozone
OC	Organic carbon
OH·	Hydroxyl radical
PAH	Polycyclic aromatic hydrocarbons
PBS	Phosphate buffered saline
PERK	Pancreatic ER kinase-like ER kinase
PM	Particulate matter
PM_{10}	Particulate matter with a mean diameter of ≤10μm
$PM_{2.5}$	Particulate matter with a mean diameter of ≤2.5μm
PRDX2	Peroxiredoxin-2
PRDX6	Peroxiredoxin-6
PS	Phosphatidylserine

RER	Rough endoplasmic reticulum
Rhod 2-AM	Rhod-2 acetoxymethyl ester
RNA-seq	RNA sequencing
ROS	Reactive oxygen species
RyR	Ryanodine receptor
S.D.	Standard deviation
SER	Smooth endoplasmic reticulum
SERCA	Sarcoplasmic/endoplasmic reticulum Ca2+ transport ATPase
SIDS	Sudden infant death syndrome
SO	Superoxide
SOD1	Superoxide Dismutase 1
SOD2	Superoxide Dismutase 2
Stat3	Signal transducer and activator of transcription 3
sXBP1	Spliced X-box binding protein 1
TLR-5	Toll like receptor 5
TNFSF10	Tumor necrosis superfamily member 10
TollIP	Toll-interacting protein
TRAF2	TNF receptor-associated factor 2
TSP	Total suspended particles
TXNRD2	Thioredoxin reductase 2
U.S.	United States
UPR	Unfolded protein response
VOC	Volatile organic carbon
WHO	World Health Organization
XBP1	X-box binding protein 1
XIAP	X-linked inhibitor or apoptosis
$\Delta\psi m$	Mitochondrial membrane potential

1.0. BACKGROUND AND INTRODUCTION

1.1. Particulate Matter Air Pollution

Ambient air pollution is a major contributor to human death and disease globally. The World Health Organization (WHO) estimates that 90% of the world's population are exposed to dangerous concentrations of air pollution, resulting in 7 million deaths annually (WHO 2016). Of the premature mortalities attributed to air pollution, 58% were due to ischemic heart disease and strokes and 18% to chronic obstructive pulmonary disease (COPD) and lower respiratory infections. Ambient air pollution is classified as a group 1 carcinogen by the International Agency for Research on Cancer (IARC) and an estimated 6% of all deaths from outdoor air pollution exposure are due to lung cancer (IARC 2013; WHO 2016).

Worldwide, particulate matter (PM) air pollution is a mixture of suspended solid and/or liquid particles (Dockery & Pope 1994; Pope 2000; Brunekreef & Holgate 2002; Pope & Dockery 2006), particle size of which is determined by its aerodynamic diameter. The aerodynamic properties of PM are important because they determine how the particles are transported in the air and human respiratory system, as well as particle source and chemical composition (WHO 2016). Coarse, or large particles, are often formed from uncontrolled combustion, dust, and biological particles, such as pollen and spores, and generally range in size from 2.5-30μm (Schwela 2000; Pope & Dockery 2006). "Thoracic" particles, or PM_{10}, are classified as particles ≤10μm in diameter and can penetrate the upper respiratory system (Dockery & Pope 1994). Fine, or "respirable" particles, are often acid condensates or photochemical secondary particles derived from

vehicle emissions, manufacturing, power generation, and agriculture and are classified as ≤2.5μm in diameter ($PM_{2.5}$; Dockery & Pope 1994; Pope 2000; Brunekreef & Holgate 2002). Upon inhalation, $PM_{2.5}$ particles can reach the alveolar regions of the lung, potentially enter the bloodstream, and be distributed to other regions in the body (Dockery & Pope 1994).

1.2. Brief History of PM Epidemiology Studies

The link between mortality and PM exposure was generally accepted in the scientific community during the 1970s, which led to the introduction of the U.S. Environmental Protection Agency's (EPA) National Ambient Air Quality Standards (NAAQS) for primary and secondary total suspended particles (TSP) in 1971. However, incomplete data and computational limitations made it difficult for researchers to attribute associations between lower PM concentrations and adverse effects on human health. Most notably were several time-series cross-sectional investigations that found associations between mortality rates and particulate air pollution in U.S. metropolitan areas (Schwartz & Marcus 1990; Fairley 1990; Schwartz 1991; Pope et al., 1992; Schwartz & Dockery 1992). The purpose of these studies was not only to evaluate the health effects and mortality of air pollution during high pollution episodes, but to also evaluate changes in daily mortality rates corresponding with daily changes in air pollution at "normal" concentrations. It was estimated that increases in daily mortality were associated with 0.5-1.5% per 10μg/m^3 increase in PM_{10} concentrations or 5-6μg/m^3 in $PM_{2.5}$ concentrations (Pope 2000). However, these studies received criticism due to lack of directly controlling for cigarette smoking or other covariates.

The landmark Harvard Six Cities Study (Dockery et al., 1993) found that mortality was strongly associated with $PM_{2.5}$ exposure after directly controlling for risk factors such as age, sex, body-mass index, cigarette smoking, education level, and occupational exposure, reporting a mortality-rate ratio of 1.26 (95% confidence interval (CI)). In epidemiology studies, a mortality-rate ratio is defined as the number of observed deaths in the study group compared to the number of expected deaths in the general population. In agreement with the earlier time-series studies, the Harvard Six Cities Study also found that $PM_{2.5}$ was most strongly associated to death from cardiopulmonary disease (mortality-rate ratio of 1.37; 95% CI). A second prospective landmark study (Pope et al., 1995) evaluated ambient air pollution data from 151 U.S. metropolitan areas and affirmed a strong association between cardiopulmonary mortality and $PM_{2.5}$ exposure after accounting for individual risk factors, reporting a relative risk ratio of 1.31 (95% CI). A relative risk ratio is often used in epidemiology studies and compares the risk of disease among the exposed group compared to unexposed group.

In addition to cardiopulmonary disease, long-term $PM_{2.5}$ exposure has also been associated with all-cause and lung cancer mortality. Another study (Pope et al., 2002) more precisely defined risk by showing that each incremental rise of $10\mu g/m^3$ in $PM_{2.5}$ was associated with a 4%, 6%, and 8% increased risk of all-cause, cardiopulmonary, and lung cancer mortality, respectively. Similarly, a Utah-based study (Archer 1990) reported that an estimated 30-40% of respiratory cancer and respiratory disease deaths in the community were associated with $PM_{2.5}$ pollution emitted by a local coal-fired steel mill. Furthermore, after controlling for maternal risk factors, PM_{10} exposure was found to be associated with post-neonatal infant all-cause, respiratory, and sudden infant death

syndrome (SIDS) mortality, reporting odds ratios of 1.10, 1.40, and 1.26, respectively (95% CI; Woodruff et al., 1997). An odds ratio is another measure of association used in epidemiology studies and quantifies the relationship between an exposure with two categories and health outcome.

Due to the growing body of evidence demonstrating a link between $PM_{2.5}$ pollution and human mortality, and a lawsuit by the American Lung Association, the EPA revised the NAAQS to amend the 1987 ruling on PM_{10} (150μg/m^3 per 24 hr and 50μg/m^3 annual for both primary and secondary PM_{10}) to include new regulatory limits on $PM_{2.5}$ pollution (EPA 2021; Pope & Dockery 2006). In 1997, the NAAQS first implemented the ruling of 65μg/m^3 and 15μg/m^3 for 24 hr and annual exposure, respectively, of primary and secondary $PM_{2.5}$. Additional data resulted in a further adjustment of the NAAQS in 2006 to 35μg/m^3 per 24 hr and 15μg/m^3 annually (EPA 2021).

Although many other countries have implemented regulatory guidelines and monitoring processes for $PM_{2.5}$ air pollution, adverse health effects associated with $PM_{2.5}$ exposure continues to be a significant problem worldwide. In addition to all-cause mortality and cardiovascular-related disease and mortality, there is a concerning emerging body of evidence suggesting that $PM_{2.5}$ exposure is also associated with neurodegenerative disease, cognitive impairment, diabetes, pneumonia, and multiple forms of cancer (Peters et al., 2006; Calderon-Garciduenas et al., 2016). In a cohort study of individuals >65 years old, a 138% increased risk of Alzheimer's disease (AD) for every 4.34μg/m^3 increase in $PM_{2.5}$ over the course of the 10-year follow-up period was found, suggesting a strong association between long-term exposure to $PM_{2.5}$ and AD development (Jung et al., 2015). Long-term $PM_{2.5}$ exposure was also found to be

associated with diabetes incidence after accounting for individual risk factors using the Cox proportional hazards models, reporting a hazard ratio of 1.11 (95% CI; Chen et al., 2013). In epidemiology studies, a hazard ratio is similar to a risk ratio but also considers the timing of the disease events associated with exposure in addition to the total number of events. $PM_{2.5}$ is also associated with bladder cancer mortality (hazard ratio of 1.13 and 1.48; 95% CI; Turner et al., 2017; Coleman et al., 2020) and breast cancer incidence (hazard ratio of 1.05; 95% CI; White et al., 2019). Additionally, a recent cohort study (Bowe et al., 2019) of 4.5 million U.S. veterans found the burden of death associated with $PM_{2.5}$ exposure was higher in predominately black and socioeconomically disadvantaged communities, with the leading causes of death being cardiovascular disease, cerebrovascular disease, chronic kidney disease, COPD, dementia, type II diabetes, lung cancer, and pneumonia.

1.3. Cache Valley Particulate Matter Air Pollution – "Cows and Cars"

The normally picturesque Cache Valley of Northern Utah is a relatively narrow valley surrounded by steep mountain ranges (Mukerjee et al., 2019). Logan is the largest city in Cache Valley and is approximately 61km long by 50km wide with an estimated 51,542 residents, while Cache Valley as a whole has an estimated 128,289 residents (U.S. Census 2019) with 99,936 registered vehicles (Utah State Tax Commission 2020). Cache Valley is also home to agricultural activities, with an estimated 57,695 cattle and calves, 2,912 horses and ponies, 2,685 sheep and lambs (U.S. Agriculture Census 2017), and 707,600 total mink pelts produced (USDA 2019). Chicken and pigs are also included in

the valley's agriculture activities, but commercial statistics were not reported in the U.S. Agriculture Census due to the low number of commercial producers.

Wintertime near-surface temperature inversions, associated with multiday stagnation events, are a common phenomenon due to the combination of snow cover, cold surface temperatures, low wind speeds, low solar radiation, and regional high pressure (Baasandorj et al., 2018; Malek et al., 2006; Silva et al., 2007; Wang et al. 2012). Consequently, air pollutants formed near the surface become trapped in the inversions and accumulate over time as the stagnant air persists, often reaching concentrations that easily exceed the current 24 hr NAAQS standard of 35μg/m^3 (Malek et al., 2006; Wang et al., 2015; Martin 2006). Cache Valley has had documented $PM_{2.5}$ concentrations that have exceeded those in Salt Lake Valley, a much larger and more populated area (Gillies et al. 2010). In January 2004, Cache Valley received national attention for achieving the nation's worst air pollution, with $PM_{2.5}$ concentrations reaching 132.5μg/m^3 and reports stating, "Logan air is the dirtiest in the USA", and "Logan air found worst to breathe in the USA" (Malek et al., 2006; The Salt Lake Tribune, 2004).

Elevated wintertime $PM_{2.5}$ concentrations in Cache Valley are primarily due to a combination of human activity and environmental factors. Abundant precursor material is predominately generated from vehicle emissions and agricultural practices, while contributing environmental factors include topography and optimal atmospheric photochemical conditions (Mangelson et al., 1997; Silva et al., 2004; Martin 2006; Silva et al., 2007; Baasandorj et al., 2018). Cache Valley's $PM_{2.5}$ (CVPM) is formed as a secondary pollutant, with the major fractions including ammonium nitrate (NH_4NO_3), organic carbon (OC), and ammonium chloride (NH_4Cl). Similar to the San Joaquin

Valley of California, NH_4NO_3 constitutes largest fraction of CVPM, which is formed by reversible acid-base reactions between gas-phase ammonia (NH_3) and nitric acid (HNO_3) precursor compounds primarily produced by activities such as animal agricultural, automobile exhaust, and wood stove combustion (Martin & Koford 2004; Malek et al., 2006; Baasandorj et al., 2018). Ammonia gas can be directly emitted from animal excreta or converted via volatilization from urea. Combustion sources, such as vehicles, power generation and industrial activity, emit nitric oxide (NO) and volatile organic carbons (VOCs) which can be oxidized by ozone (O_3) to nitrogen dioxide (NO_2) and then converted by O_3 or hydroxyl radicals ($OH\cdot$) to HNO_3 in the atmosphere. Gas-phase NH_3 and HNO_3 are able to undergo an acid-base reaction producing NH_4NO_3 salt which itself is toxicologically inert but acts as a nucleus onto which toxic atmospheric pollutants attach (Mangelson et al., 1997; Watterson et al., 2007). The formation of NH_4NO_3 is a reversible reaction that is exacerbated at low winter temperatures and builds-up during inversion events (Figure 5.1).

Emissions from vehicle sources become more prominent during the winter due to inefficient cold-starts and extended engine idling, which enhances incomplete fuel combustion and emission of NO into the air (Martin 2006; Malek et al., 2006). Ammonium nitrate generally comprises approximately 40% of CVPM particle mass but can reach 80-85% of the total mass concentration during inversion conditions (Martin 2006; Silva et al., 2007). The elevated $PM_{2.5}$ concentrations have been found to be homogenous throughout Cache Valley, and not limited to Logan and the adjacent urban areas (Martin & Koford 2004), suggesting that potential adverse health effects associated with CVPM exposure is a concern for all Cache Valley residents. Furthermore, current

estimates of future regional climate in the American West suggest that there is likely to be an increase in stagnation events, leading to a degradation of air quality in the valleys affected by inversions (Leung & Gustafson 2005; Wang et al., 2015).

Historically, Cache Valley maintained attainment status under the original 1997 24 hr NAAQS of 65μg/m^3 from 2000-2006. However, following the update of the 24 hr standard to 35μg/m^3 in 2006, the two-state area was first designated as nonattainment in 2009 based on 3-year average data. Under the EPA's guidelines to achieve attainment status, Cache County officials, the Division of Air Quality (DAQ), and the Bear River Health Department developed a plan and secured funding to reduce human-controlled emissions from vehicle, wood-burning, and local industrial sources. The area remained designated moderate nonattainment during 2008-2013, but the EPA recently modified the status of the area for the first time in 2018 to be in attainment based on monitoring data from 2015-2017.

1.4. Mechanisms of CVPM Toxicity

While it is well-documented human exposure to $PM_{2.5}$ from other locales is linked to several human diseases, the exact mechanism(s) of CVPM toxicity have yet to be fully characterized. However, preliminary and published data from our laboratory has prompted our hypothesis that CVPM activates the inflammatory response via actions of protein kinase β (Akt), a serine/threonine-specific protein kinase involved in cell survival processes and cancer cell growth, the pro-inflammatory transcription factor nuclear factor-kappa β (NF-kβ; Watterson et al., 2007; Watterson et al., 2012), and endoplasmic reticulum (ER) stress leading to activation of the unfolded protein response (UPR;

Watterson et al., 2009). Furthermore, our results correlate with mechanisms identified in similar studies using PM collected from other locales as well (Laing et al., 2010; Mendez et al., 2013; Liu et al., 2015; Velali et al., 2016; Zhou et al., 2017).

1.5. Endoplasmic Reticulum Stress

In eukaryotic cells, the ER is a membrane bound cellular organelle that is the first compartment in the secretory pathway (Hetz 2012; Chaudhari et al., 2014). The ER is characterized by a continuous extensive network of tubules, vesicles, and cisternae with several important domains, including the nuclear envelope domain, the rough endoplasmic reticulum domain (RER), smooth endoplasmic reticulum domain (SER), and contact regions with neighboring organelles, such as the plasma membrane, Golgi, vacuoles, mitochondria, peroxisomes, late endosomes, and lysosomes (Chaudhari et al., 2014).

Primary functions of the ER include N-linked glycosylation, synthesis and storage of sterols and lipids, Ca^{2+} storage, and the facilitation of proper protein folding, storage, and transport to their designated target sites in the cell (Schroder & Kaufman 2005; Hetz 2012; Bettigole & Glimcher 2015). Only correctly folded proteins can be transported to the Golgi complex for downstream modifications and packaging while incorrectly or incompletely folded proteins are retained in the ER lumen until completion of the protein folding process. If a protein cannot be properly folded then it is targeted for the endoplasmic-reticulum-associated protein degradation (ERAD) pathway, ultimately leading to retrotranslocation of the protein to the cytosol followed by proteasomal

disassembly (Schroder & Kaufman 2005; Walter & Ron 2011; Chaudhari et al., 2014; Senft & Ronai 2015).

A number of external or internal cellular perturbations resulting from exposure to environmental pollutants, such as activation of the inflammatory response, Ca^{2+} imbalances, oxidative stress, nutrient deprivation, and viral infection, can cause ER stress and a disruption of ER homeostasis, leading to the accumulation of unfolded or misfolded proteins in the ER lumen (Schroder & Kaufman 2005; Hetz 2012; Chaudhari et al., 2014; Bettigole & Glimcher 2015). Protein folding is an energy-intensive process that is interrupted in cells stressed in certain disease states or after exposure to environmental pollutants (Read & Schroder 2021). Initial adaptive mechanisms employed by the cell to restore normal physiology include enhancement of the protein folding capacity of the ER through upregulation of foldases, molecular chaperones and proteins involved in the ERAD clearance pathway, new protein synthesis downregulation, and increasing the overall size of the ER (Read & Schroder 2021). Additionally, in response to prolonged ER stress, the highly conserved UPR is initiated in the cell, which is primarily mediated by three transmembrane proteins: double-stranded RNA-activated pancreatic ER kinase-like ER kinase (PERK), activating transcription factor 6 (ATF-6), and inositol-requiring enzyme 1 (IRE1; Ron & Walter 2007; Hetz 2012).

1.6. The Unfolded Protein Response (UPR)

The UPR transmembrane proteins are initially pro-survival in nature. When the ER is in an unstressed state, the molecular chaperone immunoglobulin heavy chain binding protein (BiP/GRP78) is bound to PERK, ATF-6, and IRE1, inactivating the UPR

transducer proteins (Kozutsumi et al., 1988). Upon accumulation of unfolded or misfolded proteins in the ER lumen, BiP is sequestered and dissociates from PERK, ATF-6, and IRE1, eliciting the UPR in an attempt restore ER homeostasis (Senft & Ronai 2015). Once BiP has dissociated from PERK, the PERK protein autophosphorylates and homodimerizes, then directly phosphorylates eukaryotic initiation factor-2α (eIF2α), which functions to halt further protein translation in the ER by interfering with the 5'-cap assembly (Schroder & Kaufman 2005). BiP dissociation from IRE1 also facilitates IRE1 homodimerization and autophosphorylation, which further induces the expression of multiple proteins that are highly involved in the feedback inhibition of PERK phosphorylation, such as BCL2 antagonist/killer-1 (BAK), BCL2-associated X apoptosis regulator (BAX), BAX inhibitor-1 (BI-1), and aryl hydrocarbon receptor interacting protein-1 (AIP-1; Hetz 2012).

Unlike PERK and IRE1, BiP disengagement from ATF-6 leads to translocation of the ATF-6 protein from the ER to the Golgi complex where ATF-6 undergoes intramembrane proteolysis, producing active ATF-6 transcription factors that are subsequently released into the cytosol (Schroder & Kaufman 2005; Hetz 2012). The activated transcription factors then migrate to the cellular nucleus and elicit their response by interacting with nuclear resident transcription factors to regulate UPR gene expression to induce the transcription of proteins that are able to evade PERK-mediated translation blockage and begin to restore normal protein folding activities in the ER (Hetz 2012). However, if homeostasis cannot be sufficiently restored then the UPR essentially switches from a pro-survival to a pro-apoptotic state to eliminate the damaged cell from the population (Sovolyova et al., 2014; Szegezdi et al., 2006; Sano & Reed 2013).

1.7. Alterations in Cellular Physiology Associated with UPR Activation

In addition to the ER's primary responsibilities involving protein folding and lipid biosynthesis, the organelle also serves as the major cellular Ca^{2+} reservoir, with Ca^{2+} concentrations ranging from 1-3mM in the ER lumen (Bravo et al., 2011). The ER not only utilizes stored Ca^{2+} for protein folding activities, but also as a key component in cellular signaling events, most notably for modulation of mitochondria bioenergetics. In contrast, lower Ca^{2+} concentrations (~0.1μM) are maintained in the cytosol to facilitate the use of Ca^{2+} in alternative biological processes, such as second messengers (Bravo et al., 2011; Sovolyova et al., 2014). The normal high-to-low ratio of Ca^{2+} in the ER lumen and cytosol, respectively, is maintained through Ca^{2+} uptake into the ER via sarcoplasmic/endoplasmic reticulum Ca^{2+} transport ATPase (SERCA) pumps, and Ca^{2+} release from the ER through inositol triphosphate receptors (IP3R) and ryanodine receptors (RyR; Bravo et al., 2011; Sovolyova et al., 2014). However, current research suggests that sufficient ER stress and activation of the UPR leads to chronic depletion of Ca^{2+} from the ER to the cytosol and/or mitochondria through associated IP3Rs and RyRs (Vannuvel et al., 2013). Normal mitochondrial functions are sensitive to fluctuations in Ca^{2+} concentrations (Vannuvel et al., 2013), and unregulated release of Ca^{2+} into the mitochondria can lead to decreased energy production, mitochondrial membrane depolarization, release of cytochrome c oxidase into the cytoplasm, and eventually irreversible apoptosis (Bravo et al., 2011; Sovolyova et al., 2014).

1.8. Particulate Matter-Induced Inflammatory Response and ER Stress/UPR Crosstalk

The mechanisms underlying the wide array of PM-related diseases is the subject of intense toxicological research. The inflammatory response is a nonspecific cellular response to toxic injury or assault. Initially, during acute inflammatory responses, the release of inflammatory mediators, such as interleukins and prostaglandins, function to facilitate controlled cellular healing and repair (Xu et al., 2013; Chen et al., 2018). However, persistent injury can cause sustained upregulation of inflammatory cells and molecules which can lead to uncontrolled tissue scarring and detrimental DNA damage (Chen et al., 2018).

Endoplasmic reticulum stress is a mechanism common to many inflammatory chronic diseases, such as metabolic diseases, arthritis, cardiovascular disease, inflammatory bowel disease, atherosclerosis, neurodegenerative diseases, diabetes, and cancer (Wang & Kaufman 2012; Chaudhari et al., 2014; Grootjans et al., 2016). Multiple crosstalk nodes exist between ER stress and inflammation, suggesting that ER stress and the UPR can directly initiate inflammatory pathways in parallel with the ability of pro-inflammatory molecules to trigger ER stress (Hotamisligil 2010; Grootjans et al., 2016). It is well documented that $PM_{2.5}$ exposure triggers the inflammatory response, as evidenced by increased presence of inflammatory mediators and pro-inflammatory cytokine release, as well as the recruitment of inflammatory and immune-specific cells (Vawda et al., 2014; Pope et al., 2016). Our laboratory has revealed that CVPM-exposed human lung cells demonstrate an upregulation in cytokine and interleukin activity, as well as activation of PERK, ATF-6, and activating transcription factor 4 (ATF-4; Watterson et al., 2007; Watterson et al., 2009), in agreement with other studies (Mendez

et al., 2013; Velali et al., 2016; Li et al., 2017; Wang et al., 2017; Zhou et al., 2017; Longhin et al., 2018; Hanai et al., 2019), suggesting potential overlap between the inflammatory and UPR pathways (Figure 5.2).

1.9. Unfolded Protein Response-Related Disease States

Understanding the underlying toxic mechanisms of $PM_{2.5}$ is important because ER stress and activation of the UPR is a hallmark of many serious diseases, including diabetes, neurodegenerative disease, ophthalmic disorders, inflammation, cardiovascular disease, and cancer (Haeri & Knox 2012; Vannuvel et al., 2013; Sano & Reed 2013). There is a growing body of evidence suggesting mitochondrial dysfunction in conjunction with the ER stress response are strongly associated with insulin resistance and type II diabetes (Harding & Ron 2002; Gurzov et al., 2008; Gurzov et al., 2009; Gurzov et al., 2010). The UPR is involved in pancreatic beta cell death by overexpression of PERK, leading to downregulation of anti-apoptotic proteins, such as myeloid-cell leukemia 1 (Mcl-1), and activates C/EBP homologous protein (CHOP), which can assist with mitochondrial associated cell death. In addition, IRE1 recruitment of TNF receptor-associated factor 2 (TRAF2) subsequently activates the apoptosis signal-regulating kinase 1 (ASK1)/c-Jun N-terminal kinase (JNK) pathway, ultimately leading to cell death via the release of mitochondrial-associated apoptotic factors and executioner caspase-3 activation.

Alzheimer's disease (AD) is a common neurodegenerative disorder characterized by progressive memory impairment due to the build-up of plaques causing the massive loss of neurons in the brain (Rozpedek et al., 2015). Postmortem histopathological

experiments on the brain tissue of AD patients demonstrated a significant increase in UPR-associated markers, such as BiP, phosphorylated PERK, eIF2α, phosphorylated IRE1, spliced X-box binding protein 1 (sXBP1), and CHOP, suggesting long-term stimulation of the UPR could be strongly associated with AD neurodegenerative processes (Kudo et al., 2002; Sano & Reed 2013). Similarly, increased expression of BiP, sXBP1, ATF-4, and CHOP have been observed in patients with heart failure as consequence of increased oxidative stress and hypoxia followed by increased protein synthesis and onset of ER-stress induced UPR activation (Kadowaki & Nishitoh 2013).

Unfolded protein response activation during tumor cell growth is well documented. BiP induction contributes to tumor cell growth and proliferation (Kadowaki & Nishitoh 2013) while BiP inhibition suppresses growth, progression, and metastasis (Jamora et al., 1996). Additionally, under hypoxic conditions, PERK inactivation has been shown to impair tumor survival (Bobrovnikova-Marjon et al., 2010) and X-box binding protein (XBP1) deletion was found to reduce tumor formation (Romero-Ramirez et al., 2004), thus the UPR pathway may serve as a potential target for the treatment of cancer.

2.0. CELL CULTURE BIOASSAYS AND RNA SEQUENCING

2.1. Hypothesis

Our previous work demonstrated that CVPM exposure to BEAS-2B human bronchial epithelial cells results in increases in post-translational modifications of proteins heavily involved in ER stress and the UPR (Watterson et al., 2009). Similarly, published research has also demonstrated that exposure to $PM_{2.5}$ from other locales affects the expression of major UPR proteins and ER stress-related apoptosis markers, and well as caused an increase in oxidative stress and mitochondrial dysfunction (Malhotra et al., 2008; Vannuvel et al., 2013; Chaudari et al., 2014; Liu et al., 2015).

Therefore, my overall hypothesis is that the mechanism of cellular dysregulation and toxicity of CVPM is due, at least in part, to induction of the UPR. My hypothesis was formed, in part, based on our preliminary and published data, demonstrating that CVPM upregulates key markers involved in the UPR in cultured human lung cells. I tested this hypothesis in experiments organized into two Specific Aims.

2.2. Specific Aims

A long-term goal of this research is to understand the mechanisms involved in CVPM toxicity as a first step in assessing the risk to human health posed by exposure to this toxicant.

Aim 1. Sequence the transcriptome of BEAS-2B cells following CVPM exposure to confirm the major cellular networks that are affected. Our previous work demonstrates

there is a significant upregulation in the transcription of several proteins predominantly involved in the UPR following exposure to CVPM. However, our lab recently updated our ambient $PM_{2.5}$ collection process from a filter-based method to $PM_{2.5}$ collection onto stainless-steel disks to reduce the risk of introducing unwanted artifacts into the $PM_{2.5}$ stock and enhance the efficiency of $PM_{2.5}$ recovery. Thus, next generation RNA sequencing techniques were used to analyze the transcriptome of human bronchial cells to confirm the results from our previously published work and to test my hypothesis that the UPR is an important mechanism of CVPM toxicity. Finally, all experiments were conducted in parallel with diesel exhaust particles (DEP) to enable a firmer risk comparison because the toxic potency and resultant health effects of DEP are well known.

Aim 2. Evaluate dysregulation in human lung cell physiology following exposure to CVPM using cell culture bioassays, focusing on the UPR and other pathways identified in Aim 1. Preliminary and published data indicate that there are multiple measurable alterations in cell physiology resulting from significant ER stress and UPR induction, such as an increase in reactive oxygen species (ROS), mitochondrial dysfunction, efflux of Ca^{2+} ions from the ER, cytotoxicity, and apoptosis. For this work, I evaluated these, and other markers of the UPR and cellular dysregulation, to test my hypothesis that the UPR is an important mechanism of CVPM toxicity. As in Aim 1, all experiments also included exposure to DEP for comparison.

2.3. Experimental Approach

2.3.1. Chemicals, Reagents, and Supplies. Human bronchial (BEAS-2B) cells were generously gifted from Dr. Katerine Macé (Nestle Research Centre; Lausanne, Switzerland). LHC-9 cell culture growth medium was from Invitrogen (Camarillo, CA), 1x TrypLE Express Enzyme for cell detachment was from Gibco (Gibco; Thermo Fisher Scientific, Inc., Waltham, MA), and 1x phosphate buffered saline (PBS) was from Cytiva (Logan, UT). Thapsigargin, 2',7'-dichlorofluorescin diacetate (DCFH-DA), Fluo-3-pentaacetoxymethyl ester (Fluo-3 AM), Rhod-2 acetoxymethyl ester (Rhod-2 AM), 3,3'-dihexyloxacarbocyanine iodide ($DiOC_6$), carbonyl cyanide m-chlorophenyl hydrazone (CCCP), 30% hydrogen peroxide (H_2O_2), and Cell Counting Kit-8 (CCK-8) were obtained from MilliporeSigma (Saint Louis, MO). The Annexin-V-FLUOS labelling solution was from Roche (Mannheim, Germany). The ROS-ID Total ROS/Super Oxide detection kit was from Enzo Life Sciences, Inc. (Farmingdale, NY). The NucleoSpin RNA/Protein kit was from Macherey-Nagel (Düren, Germany). The 96-well and 12-well culture plates were from Corning (Corning, NY) and the vent-top T-25 and T-75 culture flasks were from Thermo Fisher Scientific (Waltham, MA).

2.3.2. Particle Collection and Extraction. All ambient CVPM particles were collected on campus at a secure location at Utah State University onto stainless steel discs using the Tisch Environmental (Cleves, OH) ambient non-viable Anderson cascade impactor. The body of the Tisch impaction system was placed in a protective crate with the inlet open to the atmosphere in the particle collection location and was connected to a vacuum pump operating 24 hrs during all clear days and inversion events but turned off during

any storms or fog events to maintain the integrity of the impactor and sample discs. Following the collection process, the CVPM fraction was measured by pooling and approximating the sample below the nominal 3.2µm or 1.8µm impactor stages which includes all particles ≤2.5µm. The extracted CVPM was then transferred to cell culture media and stored at -80°C until use. Diesel exhaust particles, used as a benchmark and positive control in all studies, were generously provided by Dr. Ian Gilmour of the U.S. EPA.

2.3.3. Cell Culture and Treatment. BEAS-2B cells from the same passage were grown in LHC-9 medium in culture flasks at standard biological conditions until ~80% confluency was reached. Media for the negative control (or vehicle) was replaced with fresh LHC-9 media containing no CVPM or DEP, while the media for the test conditions was replaced with fresh LHC-9 media containing 1µg/mL CVPM (i.e., particle mass per liquid media volume), 12µg/mL CVPM, 25µg/mL CVPM, 50µg/mL CVPM, 1µg/mL DEP, and 12µg/mL DEP, with five replicates per condition (N=5) in 12-well culture plates, unless otherwise specified, and incubated at 37°C for 24 hr prior to analysis. The CVPM concentrations and incubation period were chosen based previous work from our laboratory and on potential real-world exposures (Becker et al., 2005; Watterson et al., 2007; Watterson et al., 2009; Watterson et al., 2012). Prolonged ventilation in high pollution areas may lead to exposure concentrations of 50µg/mL in the lungs (Becker et al., 2005).

2.3.4. Cytotoxicity. BEAS-2B cultures (N=5) were prepared according to section 2.3.3. in clear 96-well plates. Test conditions included the negative control, 1µg/mL CVPM, 12µg/mL CVPM, 25µg/mL CVPM, 50µg/mL CVPM, 100µg/mL CVPM, 200µg/mL CVPM, 1µg/mL DEP, 12µg/mL DEP, 25µg/mL DEP, 50µg/mL DEP, 100µg/mL DEP, and 200µg/mL DEP. Following incubation, 10µL of the CCK-8 solution was added to each well and incubated per the manufacturer's instructions. Absorbance was measured at 450nm using a SpectraMax i3x microplate reader (Molecular Devices, San Jose, CA).

2.3.5. Apoptosis. BEAS-2B cultures (N=3) were prepared according to section 2.3.3. in vent-top T-25 flasks. Following incubation, the cultures were trypsinized, washed with PBS, centrifuged at 200xg for 5 min, resuspended in the Annexin-V-FLUOS labelling solution per the manufacturer's instructions and analyzed by flow cytometry with an iQue Screener Flow Cytometer (Fluorescein 488nm/518nm, Propidium Iodide 488-540nm/617nm; Sartorius, Albuquerque, NM).

2.3.6. Reactive Oxygen Species (ROS) and Superoxide (SO) Detection. BEAS-2B cultures (N=5) were prepared according to section 2.3.3. in black-well clear-bottom 96-well plates. Following incubation, the supernatant was discarded, the cells were washed with PBS, loaded with ROS/Superoxide Detection Solution per the manufacturer's instructions, and incubated at 37°C for 1 hr. Fluorescence was measured using a SpectraMax i3x microplate reader (Fluorescein 488nm/520nm, Rhodamine 550nm/610nm). Pyocyanin is a potent ROS inducer and was included in the ROS-ID Total ROS/Superoxide Detection Kit as the ROS positive control.

2.3.7. Mitochondrial Ca^{2+} Measurement. BEAS-2B cultures (N=5) were prepared according to section 2.3.3. Following incubation, a final concentration of 10µM of Rhod-2 AM (Brisac et al., 2010) was added to each test culture well and incubated at 37°C for 30 min. The cultures were then washed with PBS, trypsinized, centrifuged at 200xg for 5 min, resuspended in PBS, and immediately analyzed by flow cytometry with an iQue Screener Flow Cytometer (552nm excitation/581nm emission). The Rhod-2 AM probe has a net positive charge and is membrane permeable, allowing it to be readily sequestered into the mitochondria. Once in the mitochondria, the AM portion is rapidly cleaved and the remaining Rhod-2 indicator fluoresces upon the binding of Ca^{2+} ions (Brisac et al., 2010).

2.3.8. Cytosolic Ca^{2+} Measurement. BEAS-2B cultures (N=5) were prepared according to section 2.3.3. Following incubation, a final concentration of 1µM of Fluo-3 AM (Brisac et al., 2010) was added to each test culture well and incubated at 37°C for 2 hr. The cultures were then washed with PBS, trypsinized, centrifuged at 200xg for 5 min, resuspended in PBS, and immediately analyzed by flow cytometry with an iQue Screener Flow Cytometer (506nm excitation/526nm emission). Fluo-3 AM is membrane permeant and is cleaved to Fluo-3 in the cytoplasm by non-specific esterases. Fluo-3 is essentially non-fluorescent unless it is bound to Ca^{2+} ions, and the fluorescent intensity increases in correspondence with an increase in Ca^{2+} concentration (Brisac et al., 2010). Thapsigargin (5µM), a potent inhibitor of the SERCA pump that causes ER stress and autophagy in mammalian cells, was used as a positive control.

2.3.9. Assessment of Mitochondrial Membrane Potential (Δψm) Drop. BEAS-2B cultures (N=5) were prepared according to section 2.3.3. Following incubation, a final concentration of 50nM (Brisac et al., 2010) of the lipophilic potential-sensitive fluorescent probe $DiOC_6$ was added to each test culture well and incubated at 37°C for 30 min. The cultures were then washed with PBS, trypsinized, centrifuged at 200xg for 5 min, resuspended in PBS, and immediately analyzed by flow cytometry with an iQue Screener Flow Cytometer (484nm excitation/501nm emission). CCCP (50µM), a chemical inhibitor of oxidative phosphorylation, was used as the positive control (Sivandzade et al., 2019).

2.3.10. RNA Purification and RNA Sequencing Transcriptomics. BEAS-2B cultures (N=3) were prepared according to section 2.3.3. in T-75 vent-top culture flasks. Test conditions included a negative control, 1µg/mL CVPM, 12µg/mL CVPM, 1µg/mL DEP, and 12µg/mL DEP. Following incubation, the cultures were trypsinized, washed with PBS, and centrifuged at 200xg for 5 min. RNA purification was immediately performed using the NucleoSpin RNA/Protein kit. Highly pure RNA samples were achieved per the NucleoSpin RNA purification protocol, which were flash-frozen in liquid nitrogen and then stored at -80°C until RNA sequencing (RNA-seq). Whole transcriptome RNA-seq was performed using an Illumina NextSeq 550 sequencer (Illumina, San Diego, CA) at Utah State University's Center for Integrated Biosystems. Only two replicates in the negative control group were included because the RNA for the third replicate had degraded during the sequencing process and was therefore eliminated from the dataset.

Individual RNA-seq reads were first mapped to the human genome (hg38) using HISAT2 version 2.1.0 (Johns Hopkins University Center for Computational Biology, Baltimore, MA; Kim et al., 2015), followed by quantification of the raw read counts using the featureCounts Bioconductor R package (Liao et al., 2014). Data pre-processing and differential expression (DE) was performed using edgeR and Limma Bioconductor R packages (Law et al., 2018). By default, significance was defined using a 5% adjusted p-value cutoff (False discovery rate (FDR) = 0.05). Pathway analysis on the DE transcripts was completed using the Ensemble Gene Set Enrichment (EGSEA; Alhamdoosh et al., 2017) Bioconductor R package, which generated the top 50 "hallmark" significantly affected pathways from the Molecular Signatures Database (MSigDB; Liberzon et al., 2015). The EGSEA Bioconductor R package combined the FDR adjusted p-values from twelve different gene set enrichment (GSE) methods (i.e., ora, globaltest, plague, safe, zscore, gage, ssgsea, padog, gsva, camera, roast, and fry) using the Wilkinson method and ranked them using the median.

2.3.11. Statistical Analysis. All statistical analysis was performed using JMP, version 15 (SAS, Cary, NC), with Tukey adjustments for multiple *post hoc* comparisons.

2.4. Results

2.4.1. Cytotoxicity and Apoptosis. Both particle types were significantly more cytotoxic than the negative control at concentrations ≥50µg/mL (Figure 5.3). However, at ≥100µg/mL DEP was significantly more cytotoxic than CVPM. EC_{50}'s of 441µg/mL and 259µg/mL for CVPM and DEP, respectively, were extrapolated using line fitting with

simple linear regression. Cellular measurement of EC_{50} for CVPM was not possible because the maximum stock concentration of collected CVPM (~200µg/mL) was insufficiently cytotoxic to achieve 50% cytotoxicity.

Apoptosis can be triggered by various stimuli, such as a loss of mitochondrial membrane potential ($\Delta\psi m$), leading to the release of pro-apoptotic signaling compounds from the mitochondria into the cytoplasm (Alirol et al., 2006; Vannuvel et al., 2013). Apoptotic events were measured at the membrane using the fluorescent probes Annexin V and propidium iodide. First, apoptosis-activated translocation of phosphatidylserine (PS) to the external surface of the cell was quantified with Annexin V which binds to PS. Propidium iodide acts as a necrotic cell DNA fluorescent probe to discriminate between necrotic and apoptotic cells: cells that exclude either Annexin V or propidium iodide are considered alive, while those that bind primarily to propidium iodide are considered necrotic. Additionally, cells that bind primarily to Annexin V are considered early in apoptosis, while those that take up both Annexin V and propidium iodide are both apoptotic and necrotic, thus later-stage apoptosis.

In this work, there appeared to be a concentration-related increase in necrotic cells corresponding to an increase in CVPM concentration and treatment with ≥12µg/mL CVPM was significant from both the negative control (73.5%, 121.9%, and 462.9% increases for 12µg/mL CVPM, 25µg/mL CVPM, and 50µg/mL CVPM, respectively) and equivalently tested concentrations of DEP (133.6% increase for 12µg/mL CVPM; Figure 5.4). Exposure to 12µg/mL CVPM also caused a significant increase in cells in late-stage apoptosis compared to the negative control (24.7% increase for 12µg/mL CVPM) but there was no significant difference between CVPM and DEP at equivalent

concentrations. At all tested concentrations, CVPM treatment did not cause a significant increase in early apoptosis events compared to the negative control and 12µg/mL DEP exposure resulted in a significant increase in cells in early apoptosis compared to 12µg/mL CVPM (618% increase for 12µg/mL DEP).

2.4.2. Reactive Oxygen Species (ROS) and Superoxide (SO). Cellular oxidative stress mediated by ROS formation is believed to play an important role in $PM_{2.5}$ toxicity (Xia et al., 2007; Zhou et al., 2017; Vattanasit et al., 2014). Oxidative injury can damage the ER membrane and subsequent secretory protein folding, leading to ER stress and activation of the UPR (Rashid et al., 2015). At the concentrations tested, CVPM appeared to induce a concentration-related increase in ROS production; CVPM (at 50µg/mL) elicited a significant increase compared to negative control (18.3% increase for 50µg/mL CVPM; Figure 5.5). Generation of SO was also associated with CVPM treatment, but not to a degree that was statistically significant. Cells treated with DEP had significant increases in both ROS and SO compared to the negative control (18.6% increase in ROS for 12µg/mL DEP; 23.6% increase in SO for 1µg/mL DEP), but these markers of free-radical generation were not different from that in CVPM-treated cultures.

2.4.3. Ca^{2+} Imbalances. Another consequence of ER stress and UPR activation is an efflux of Ca^{2+} ions from the ER lumen into the cytoplasm (Vannuvel et al., 2013) with the resultant gradient causing an influx into the mitochondria (Sovolyova et al., 2014). In our study, cultures treated with CVPM showed concentration-related increases in both cytosolic and mitochondrial Ca^{2+} concentrations compared to the negative control (55.3%

and 120.8% increase in cytosolic Ca^{2+} for 25µg/mL CVPM and 50µg/mL CVPM, respectively; 33.1%, 31.6%, 39.8%, and 77.9% increase in mitochondrial Ca^{2+} for 1µg/mL CVPM, 12µg/mL CVPM, 25µg/mL CVPM, and 50µg/mL CVPM, respectively; Figure 5.6). In both experiments, treatment with 12µg/mL DEP caused a significant increase in intracellular Ca^{2+} concentrations compared with same concentration of CVPM (214.2% and 68.9% increase in cytosolic and mitochondrial Ca^{2+} for 12µg/mL DEP, respectively).

2.4.4. Assessment of Mitochondrial Membrane Potential (Δψm) Drop. Decreases in Δψm is an important parameter of mitochondrial functional, as well as overall cellular viability (Vannuvel et al., 2013). Investigating dysregulation in mitochondrial physiology in relation to CVPM toxicity via the UPR is important because following sufficient ER stress, Ca^{2+} ions are released from the ER to the mitochondria through voltage gated Ca^{2+} channels in the mitochondrial associated membranes (MAMs; Vannuvel et al., 2013; Bhat et al., 2017; Senft & Ronai 2015). An efflux of Ca^{2+} from the ER to the mitochondria causes a loss of Δψm, which can lead to release of cytochrome c oxidase from the mitochondria into the cytoplasm indicating the cell is transitioning towards apoptosis. In this study, significant concentration-related decreases in Δψm were observed for all CVPM treated conditions compared to the negative control (34.4%, 43.1%, 73.9%, and 127.9% drop in Δψm for 1µg/mL CVPM, 12µg/mL CVPM, 25µg/mL CVPM, and 50µg/mL CVPM, respectively; Figure 5.7). Treatment with 12µg/mL DEP caused a significant loss of Δψm compared to 12µg/mL CVPM (137.2% drop in Δψm for

12µg/mL DEP), but there was no significant difference in Δψm between 1µg/mL CVPM and 1µg/mL DEP.

2.4.5. Transcriptomic Differential Expression (DE) and Pathway Analysis. Differential expression analysis on the RNA-seq count data was completed with edgeR and Limma Bioconductor packages (see section 2.3.11). At 1µg/mL, CVPM and DEP independently affected 858 and 694 genes, respectively, with 2024 similarly affected genes (FDR=0.05; Figure 5.8 and Figure 5.9). At 12µg/mL, CVPM and DEP induced 294 and 1551 independently affected genes, respectively, with 1996 similarly affected genes (FDR=0.05; Figure 5.8 and Figure 5.9).

The majority of the known genes in the hallmark UPR pathway were significantly upregulated at higher (i.e., 12µg/mL) CVPM but downregulated for lower (i.e., 1µg/mL) concentrations of CVPM (Figure 5.10), while DEP exposure caused a more marked upregulation in the UPR pathway than CVPM at equivalently tested concentrations (FDR=0.05; p=0.007 for 12µg/mL CVPM, p=0.0001 for 12µg/mL DEP). The corresponding log-fold change (logFC) directions for UPR genes of interest is shown in Figure 5.11. In this study, CVPM exposure caused a downregulation of the three primary UPR transducer genes: PERK, IRE1, and ATF-6. At 1µg/mL, CVPM exposure caused a more significant downregulation for only ATF-6 (FDR=0.05; p=0.048 for 1µg/mL CVPM, p=0.086 for 1µg/mL DEP), while DEP exposure elicited a more significant downregulation for IRE1 (FDR=0.05; p=0.022 for 1µg/mL CVPM, p=0.012 for 1µg/mL DEP), and both particle types incited a similar response for PERK (FDR=0.05; p=0.143 for 1µg/mL CVPM, p=0.143 for 1µg/mL DEP). At 12µg/mL, CVPM exposure caused a

more significant downregulation for only PERK (FDR=0.05; p=0.046 for 12µg/mL CVPM, p=0.239 for 12µg/mL DEP), while DEP exposure elicited a more significant downregulation for both ATF-6 (FDR=0.05; p=0.153 for 12µg/mL CVPM, p=0.03 for 12µg/mL DEP) and IRE1 (FDR=0.05; p=0.014 for 12µg/mL CVPM, p=0.002 for 12µg/mL DEP).

At all tested concentrations, CVPM caused an upregulation of the ER chaperone calreticulin (CALR), while only 12µg/mL CVPM caused upregulation of the ER chaperone glucose-regulated protein 94 (GRP94/HSP90B1), which are downstream effectors of ATF-6 activation. At equivalent concentrations, DEP exposure caused a greater degree of upregulation of both HSP90B1 (FDR=0.05; p=0.999 for 1µg/mL CVPM, p=0.201 for 1µg/mL DEP, p=0.309 for 12µg/mL CVPM, p=0.202 for 12µg/mL DEP) and CALR, while only 12µg/mL DEP for CALR was significant (FDR=0.05; p=0.376 for 1µg/mL CVPM, p=0.098 for 1µg/mL DEP, p=0.146 for 12µg/mL CVPM, p=0.036 for 12µg/mL DEP).

Although not significant, a major downstream effector of the UPR transducer protein IRE1, XBP1, was upregulated across all tested CVPM concentrations. XBP1 assists in UPR regulation by mediating cellular adaptation to ER stress, leading to the transcription of ER chaperone proteins (Ron & Walter 2007). At 1µg/mL, DEP exposure caused a downregulation of XBP1 compared to CVPM (FDR=0.05; p=0.680 for 1µg/mL CVPM, p=0.669 for 1µg/mL DEP) and 12µg/mL CVPM and DEP exposure induced similar XBP1 expression (FDR=0.05; p=0.875 for 12µg/mL CVPM, p=0.877 for 12µg/mL DEP).

Following UPR initiation and PERK phosphorylation, eIF2α is subsequently activated via phosphorylation, which functions to further attenuate global protein translation in the ER in parallel with preferential translation of ATF-4, a master regulator that is highly involved in the transcription of genes related to adaptation and apoptosis (Schroder & Kaufman 2005; B'chir et al., 2013). BEAS-2B cells treated with CVPM caused a significant downregulation of eIF2α and significant upregulation of ATF-4. At equivalent concentrations, exposure to 1µg/mL CVPM elicited a more significant change in eIF2α (FDR=0.05; p=0.03 for 1µg/mL CVPM, p=0.062 for 1µg/mL DEP) and ATF-4 (FDR=0.05; p=0.003 for 1µg/mL CVPM, p=0.033 for 1µg/mL DEP) compared to DEP. However, 12µg/mL DEP caused a more significant response in both eIF2α (FDR=0.05; p=0.061 for 12µg/mL CVPM, p=0.008 for 12µg/mL DEP) and ATF-4 (FDR=0.05; p=0.014 for 12µg/mL CVPM, p=0.002 for 12µg/mL DEP) compared to CVPM.

Other significantly affected biological pathways of interest following CVPM treatment related to the UPR included upregulation of apoptosis (FDR=0.05; p=0.015 for 12µg/mL CVPM, p=0.00008 for 12µg/mL DEP; p=0.686 for 1µg/mL CVPM, p=0.188 for 1µg/mL DEP; Figure 5.10.) and ROS (FDR=0.05; p=0.007 for 12µg/mL CVPM, p=0.00006 for 12µg/mL DEP; p=0.025 for 1µg/mL CVPM, p=0.002 for 1µg/mL DEP; Figure 5.10.), as well as downregulation of the inflammatory response (FDR=0.05; p=0.004 for 12µg/mL CVPM, p=0.00005 for 12µg/mL DEP; p=0.006 for 1µg/mL CVPM, p=0.002 for 1µg/mL DEP; Figure 5.10.), with DEP causing a more significant response compared to CVPM at all equivalently tested concentrations. The corresponding logFC directions for the apoptosis, ROS, and inflammatory response pathway genes of interest are shown in Figure 5.12, Figure 5.13, and Figure 5.14, respectively.

2.5. Discussion

Cache Valley Utah has had a history of experiencing some of the highest $PM_{2.5}$ concentrations in the United States (Malek et al., 2006; USA-Today 2005). Exposure to $PM_{2.5}$ is linked to several human diseases but the exact mechanisms of CVPM toxicity have yet to be fully characterized. In a previous investigation, we hypothesized that CVPM activates ER stress and the UPR, a highly conserved cellular stress response (Watterson et al., 2009). That study involved CVPM collection onto Teflon filters which underwent an extensive aqueous extraction process possibly altering particle chemistry, or interfered with complete CVPM recovery, before cell treatment. Here, we confirm this hypothesis using a more efficient particle collection and recovery system that preserves particle chemistry and distribution until use.

A central role of the UPR in $PM_{2.5}$ pathology was subsequently confirmed by other laboratories (Laing et al., 2010; Mendez et al., 2013; Liu et a., 2015; Velali et al., 2016; Zhou et al., 2017, Xu et al., 2017, Liu et al., 2021). In the present study, CVPM induced classical markers of ER stress and UPR activation in exposed BEAS-2B cells: apoptosis, intracellular Ca^{2+} imbalances, and $\Delta\psi m$ drop, and DE of PERK, IRE1, and ATF-6 and their downstream effectors.

Initial UPR functions are pro-survival in nature. However, pro-apoptotic signaling may follow chronic and/or irreversible stress (Sovolyova et al., 2014; Szegezdi et al., 2006; Sano & Reed 2013). $PM_{2.5}$-induced apoptosis has been observed in human lung cells (Liu et al., 2015; Zhou et al., 2017) and previous work from our laboratory demonstrated CVPM exposure caused significant increases in markers related to apoptosis, such as calpain and caspase-12 activation (Watterson et al., 2007; Watterson et

al., 2009). In this study, flow cytometry revealed that CVPM exposure caused late-stage apoptosis and necrosis in human lung cells. Similar findings have been reported (Zhou et al., 2017; Zhou et al., 2017; Wang et al., 2021), suggesting that exposure to high concentrations of $PM_{2.5}$ may result in autophagy-dependent cell necrosis triggering acute inflammatory response signals. Additionally, mitochondrial oxidative stress and disruption of the electron transport chain via loss of $\Delta\psi m$ has also been postulated to be responsible for $PM_{2.5}$-associated cellular apoptosis and necrosis (Li et al., 2008; Longhin et al., 2013).

ROS-mediated oxidative stress is believed to have a crucial role in $PM_{2.5}$-mediated toxicity (Xia et al., 2007), including ROS being a key modulator of ER stress and UPR activation, likely through PERK stimulation and/or activation of the inflammatory response (Laing et al., 2010). Nevertheless, statistically significant increases in ROS production were observed at only the highest tested CVPM concentration. The lack of detectible ROS with <50µg/mL CVPM treatment is likely a reflection of the low concentration of ROS-inducing transition metals, like iron, compared to $PM_{2.5}$ from other locales (Mangelson et al., 1997; Watterson et al., 2007; Baasandorj et al., 2018). Iron is an essential constituent of the Fenton reaction, which produces reactive species capable of oxidizing biological molecules from hydrogen peroxide and ferrous salt substrates (Winterbourn 1995). Due to the growing body of evidence suggesting $PM_{2.5}$-related reactive species are strong activators of the UPR, future work in this area may include a more targeted investigation of potential CVPM-related reactive species, including specific ROSs (i.e., SO, H_2O_2, HO·, and NO), lipid peroxides, and reduced glutathione.

In this study, flow cytometry experiments revealed that CVPM treatment caused a significant efflux of both cytosolic and mitochondrial Ca^{2+}. Perturbations of Ca^{2+} homeostasis related to UPR activation is an established response to PM exposure in J774 murine macrophage and human peripheral blood mononuclear cells (Brown et al., 2004; Brown et al., 2007). ER-stress and UPR-induced Ca^{2+} fluctuations have also been documented in human neuroblastoma IMR5 cells exposed to Poliovirus. (Brisac et al., 2010), suggesting that mitochondrial uptake of Ca^{2+} from the cytosol through the Ca^{2+} uniporter and from the ER via the IP3R and RyR channels leads to mitochondrial-induced apoptosis (Brisac et al., 2010). Similarly, $PM_{2.5}$-induced intracellular Ca^{2+} fluctuation from IP3R, RyR, and calmodulin (CAM) modulation in human Jurkat T cells has also been reported (Zhao et al., 2019). Although we observed significant alterations in cytosolic and mitochondrial Ca^{2+}, ion movement through specific Ca^{2+} channels were not investigated. Concomitant with perturbations in mitochondrial Ca^{2+}, CVPM caused a disruption in $\Delta\psi m$, another marker of ER stress and UPR activation (Brisac et al., 2010; Longhin et al., 2013). Similar $PM_{2.5}$-induced mitochondrial dysfunction in BEAS-2B cells via $\Delta\psi m$ loss, morphology changes, and respiration disruption has been reported as well (Liu et al., 2020; Sotty 2020; Leclercq et al., 2018).

Transcriptomics confirmed that CVPM exposure caused an overall significant upregulation of the UPR and related pathways, including apoptosis and ROS. While in this study CVPM exposure caused a significant downregulation of the three primary UPR transducer genes, PERK, IRE1, and ATF-6, direct downstream effectors were significantly upregulated. These results suggest activation of the UPR in BEAS-2B cells from 24 hr CVPM exposure has likely advanced beyond PERK, IRE1, and/or ATF-6

activation alone. Phosphorylation of eIF2α following PERK oligomerization and autophosphorylation due to unfolded or misfolded protein accumulation in the ER promotes the transcription of ATF-4 followed by CHOP (Hu et al., 2019). Here, we observed that CVPM significantly upregulated ATF-4 and CHOP across all CVPM test conditions. These results agree with previous work from our laboratory (Watterson et a., 2009) and others where $PM_{2.5}$ exposure has been shown to differentially affect the PERK signaling pathway (Laing et al., 2010).

CHOP is a transcription factor and a cellular stress sensor with both pro-apoptotic and anti-apoptotic gene targets (Yang et al., 2017). Canonically, overexpression of CHOP due to ER stress and the UPR has been attributed to cell cycle arrest and apoptosis predominantly via the PERK signaling pathway, most notably through pro-apoptotic signals (Marciniak et al., 2004; Li et al., 2014). CVPM exposure caused a significant upregulation of both BAX and growth arrest and DNA damage inducible β (GADD45B) in addition to CHOP, suggesting CVPM caused sufficient ER stress to promote pro-apoptotic UPR signaling pathways, likely through CHOP. The observation of late-stage apoptosis in CVPM-treated cells confirms these results.

CHOP activation is not limited to the PERK branch of the UPR alone but can occur through ATF-6 and IRE1 as well (Li et al., 2014). Activation of ATF-6 in response to ER stress is often considered a pro-survival UPR cellular mechanism and functions by binding to the promoters of genes involved in the augmentation of ER size and protein-folding capacity, including resident ER chaperones (Rutkowski et al., 2006; Hu et al., 2019). In agreement with our published data (Watterson et al., 2009), CVPM exposure caused an upregulation the ER resident chaperones heat shock protein 90kDa (HSP90)

and heat shock protein β-1 (HSPB1), although in this study only HSPB1 was significant. ATF-6 further regulates pro-survival functions of the UPR through promotion of XBP1 and CHOP (Li et al., 2014; Hu et al., 2019). XBP1 has been shown to independently activate CHOP, indicating that ATF-6 can cooperate with XBP1 to activate CHOP to promote cell survival (Hu et al., 2019). While this study demonstrated that CVPM exposure caused a significant downregulation of ATF-6 and IRE1, subsequent XBP1 upregulation was not significant indicating that CHOP activation likely occurred through the PERK/eIF2α/ATF-4/CHOP pathway or through ATF-6 and/or IRE1 independent of XBP1.

It is well documented that $PM_{2.5}$ exposure to human lung cells triggers the inflammatory response (Vawda et al., 2014; Pope et al., 2016), and substantial evidence suggests intracellular signaling overlap between the UPR and inflammatory response pathways (Hotamisligil 2010; Grootjans et al., 2016). In our previous studies (Watterson et al., 2007), microarray analysis and immunoblots detected an upregulation of inflammatory response related genes (i.e., MHC class I polypeptide-related sequence A (MICA), interleukin 1 receptor type 1 (IL1-R1), interleukin 6 receptor (IL-6R), interleukin 20 (IL-20), Toll-like receptor 5 (TLR-5), caspase-3, and Toll-interacting protein (TollIP)), and proteins (i.e., IL-6R, interleukin 6 (IL-6), signal transducer and activator of transcription 3 (Stat3), IL-1R1, interleukin 1 receptor-associated kinase (IRAK), heat shock protein 70kDa (Hsp70), and NF-κβ), respectively. It was surprising therefore that our pathway analysis showed a general downregulation of the inflammatory response pathway across all treatments. Significant DE was not observed for IL-6, interleukin 8 (IL-8), or NF-κβ, inflammatory markers well documented to be

affected by $PM_{2.5}$ exposure (Becker et al., 2005; Manzano-Leon et al., 2016). However, significant upregulation of other key proinflammatory mediators, such as 26S proteasomal ubiquitin receptor (ADRM1), interleukin 18 (IL-18), fractalkine/chemokine (C-X3-C motif) ligand 1 (CX3CL1), and interferon-induced transmembrane protein 1 (IFITM1) were detected, illustrating the complexity of the inflammatory response and UPR crosstalk. Possible explanations for the lack of detectable inflammatory markers include biased RNA-seq results, protein post-transcriptional modifications that are captured in the Western blots and not the mRNA or differing molecule half-lives leading to unproportioned mRNA and protein concentrations (Greenbaum et al., 2003; Wang et al., 2008). However, more work needs to be completed in this area before final conclusions can be made. Additionally, while the UPR was identified here as a primary mechanism of CVPM toxicity, RNA-seq revealed a significant upregulation in the DNA repair, interferon α response, and p53 pathways, which are also closely interrelated with the UPR and inflammatory response (Cooks et al., 2014; Kawanishi et al., 2017) and likely contribute to CVPM toxicity.

Compared to CVPM, DEP was generally more potent in inducing markers of ER stress and the UPR in BEAS-2B cells (Jung et al., 2007) and in most experiments, 1μg/mL DEP elicited similar results to 12μg/mL CVPM. While still hazardous to human health, the decreased toxicity of CVPM compared to DEP is most likely a reflection of differences in particle chemistry. DEP is a complex mixture of carbon, metal, and metal-oxides, in gaseous, liquid, and particulate states, with particle aggregates ranging from 10-100nm in diameter that are not easily removed from the lung (Steiner et al., 2016). DEP itself also contains many known and potent ROS species, such as ozone and NO_2,

and toxic polycyclic aromatic hydrocarbons (PAHs), like benzo-a-pyrene, that cause genotoxicity and cancer (Ferguson & Denny 2007; Steiner et al., 2016). In contrast, CVPM, while only partially characterized, is largely comprised of less toxic secondary nitrate salts, such as NH_4NO_3 (Martin & Koford 2005; Watterson et al., 2007; Baasandorj et al., 2018), which thus, at least partially, contributes to the decreased toxicity of CVPM compared to DEP at equivalent concentrations. NH_4NO_3 generally comprises around 40% of the total mass of CVPM but can reach as high as 80-85% during inversion events, indicating that only the components comprising the remaining 15-60% of CVPM are responsible for the toxic effects of CVPM exposure to human lung cells observed in this study.

In total, our results support the hypothesis that ER stress and the UPR is an important molecular mechanism of CVPM pathology. Confirmation of the UPR as an operative mechanism of $PM_{2.5}$ toxicity enhances our understanding of pollutant toxicology because activation of the UPR resulting from ER stress has been associated with the pathophysiology of many serious diseases, such as cardiovascular disease, diabetes, retinal degeneration, AD, metabolic disease, and even cancer.

3.0. ADDITIONAL RESEARCH IMPLICATIONS

3.1. Ambient $PM_{2.5}$ Human Exposure Estimations

The CVPM concentrations that BEAS-2B cells were exposed to in this study were higher than one-time exposures in most ambient settings for humans. However, the tested concentrations may be reached in humans following exposure to highly polluted areas, such as some metropolitan areas or natural disasters (Tan et al., 2000; Becker et al., 2005; Watterson et al., 2012). Assuming the volume of the epithelial lining is 20-40mL (Rennard et al., 1986) and a person ventilates 30L/min during 1 hr of exercise, then the concentration of CVPM to which human lung cells could be exposed to *in vivo* on Good, Moderate, Unhealthy for Sensitive Groups, Unhealthy, Very Unhealthy, and Hazardous, according to the EPA's 24 hr average Air Quality Index (AQI) are shown in Table 4.1.

3.2. Expanded Research Significance Based on CVPM Composition

Cache Valley, Salt Lake Valley, and Utah Valley, which are located along Utah's Wasatch Mountain range and contain an estimated 2.4 million residents (U.S. Census 2019), frequently experience some of the highest $PM_{2.5}$ concentrations in the United States during wintertime inversions. The principal component of Utah's $PM_{2.5}$ is NH_4NO_3, the formation of which is described previously in section 1.3. Aside from NH_4NO_3, CVPM is chemically distinct from $PM_{2.5}$ in Salt Lake Valley and Utah Valley, both of which have greater populations, higher vehicle traffic, and are home to steel and smelting industries that are not present in Cache Valley. However, CVPM is similar in composition to that found the San Juaquin Valley of California, which is home to 4.3

million residents and encompasses 11% of the state's population (Watterson et al., 2012; U.S. Census 2019; Lurmann et al., 2006). Therefore, our findings that CVPM exposure activates markers of the UPR in human lung cells, which is a common event in many disease states, is not only important for understanding the potential health effects of this toxicant for Cache Valley residents but for California residents as well.

3.3. Methods to Improve Air Quality for Cache Valley Citizens

Elevated wintertime $PM_{2.5}$ concentrations are a common event in Cache Valley and the potential health effects associated with $PM_{2.5}$ exposure are a concern for all Cache Valley residents. CVPM formation is a due to a combination of human activities as well as the environment, as described in section 1.3. Cache Valley citizens can help protect themselves and improve air quality by staying indoors during high pollution episodes, complete vehicle emissions testing to reduce VOCs and NOx in the atmosphere, reduce driving and engine idling during inversion events, encourage electric vehicles, and reduce agriculture and/or improve agriculture nutrition (Martin et al., 2016).

4.0.TABLES

Air Quality Index (AQI)	**$PM_{2.5}$**	**Human Lung Cell Exposure Concentration**
Good	12.0 µg/m^3	1.08 µg/mL
Moderate	35.4 µg/m^3	3.19 µg/mL
Unhealthy for Sensitive Groups	55.4 µg/m^3	4.99 µg/mL
Unhealthy	150.4 µg/m^3	13.54 µg/mL
Very Unhealthy	250.4 µg/m^3	22.54 µg/mL
Hazardous	≥ 250.5 µg/m^3	≥ 22.55 µg/mL

Table 4.1. Human lung cell ambient outdoor $PM_{2.5}$ estimated exposure scenarios, assuming the volume of the epithelial lining is 20mL and a person exercises at 30L/min of ventilation for 1 hr.

5.0. FIGURES

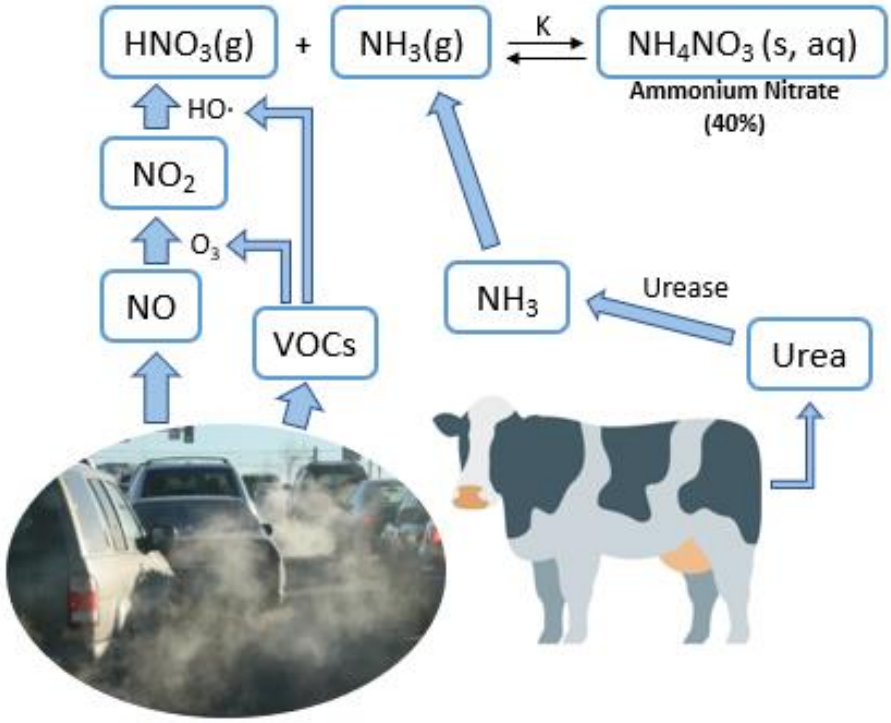

Figure 5.1. "Cows and cars". Nitric oxide and VOCs are emitted predominantly via human-controlled sources, such as vehicle tailpipe emissions, and converted to gas-phase HNO_3. Ammonia gas, also primarily produced from human-controlled animal agriculture activities, can combine with HNO_3 in the air to produce NH_4NO_3 from a reversible acid-base reaction that is exacerbated at low winter temperatures and builds up during inversion events. Ammonium nitrate comprises about 40% of the mass of CVPM, and itself is toxicologically inert but instead acts as a nuclease onto which toxic compounds attach.

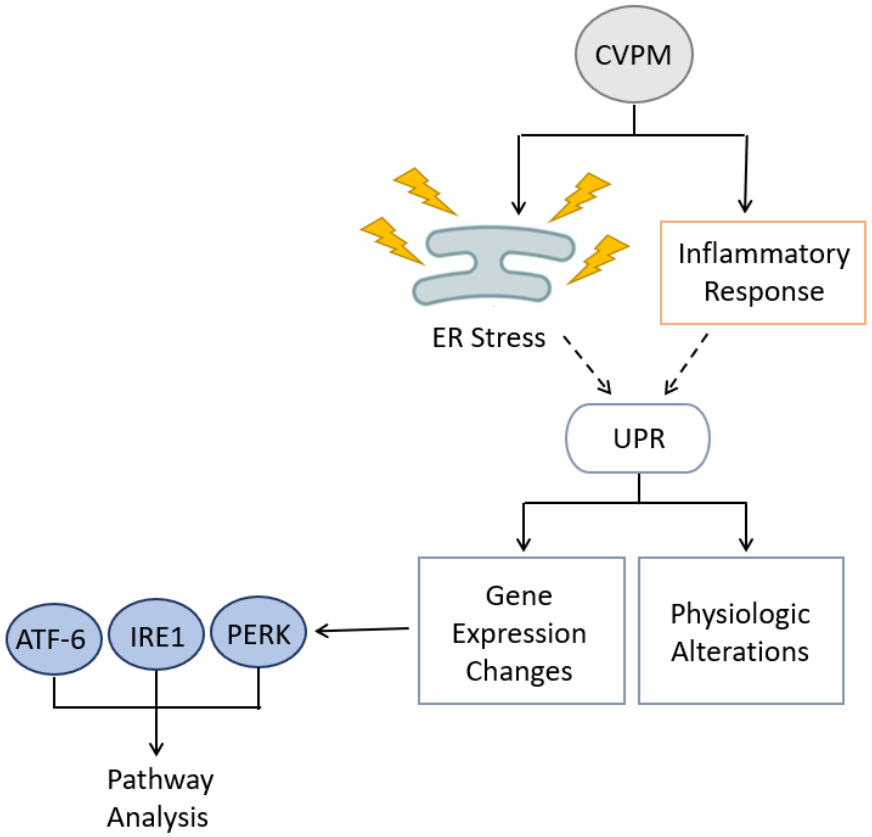

Figure 5.2. UPR and inflammatory response crosstalk. CVPM potentially leads to UPR activation via crosstalk between ER stress and the inflammatory pathways (dashed arrows), which subsequently leads to both genetic expression and physiologic cellular alterations. Gene expression changes include modulation of the UPR transducer proteins, such as PERK, IRE1, and ATF-6, while physiologic alterations involve mitochondria dysregulation, Ca^{2+} imbalances, cytotoxicity, and apoptosis.

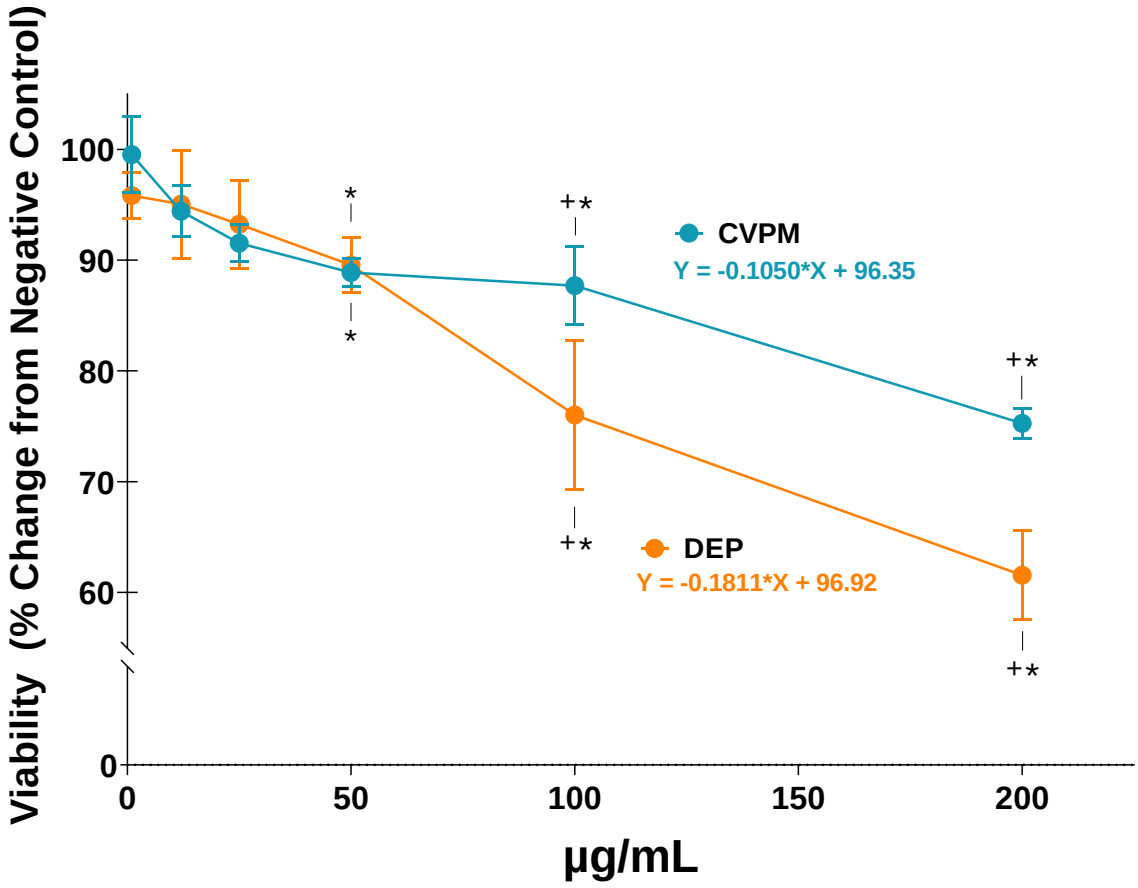

Figure 5.3. CVPM cytotoxicity assay results. DEP is substantially more cytotoxic than CVPM to human lung (BEAS-2B) cells (24 hr exposure; N=5) at ≥50µg/mL exposure concentrations using the CCK-8 assay. * = significant from the negative control and + = significant from particle type of equivalent concentration ($p \leq 0.05$ +/- 1 SD). Extrapolated simple linear regression resulted in EC_{50} values of 441µg/mL and 259µg/mL for CVPM and DEP, respectively.

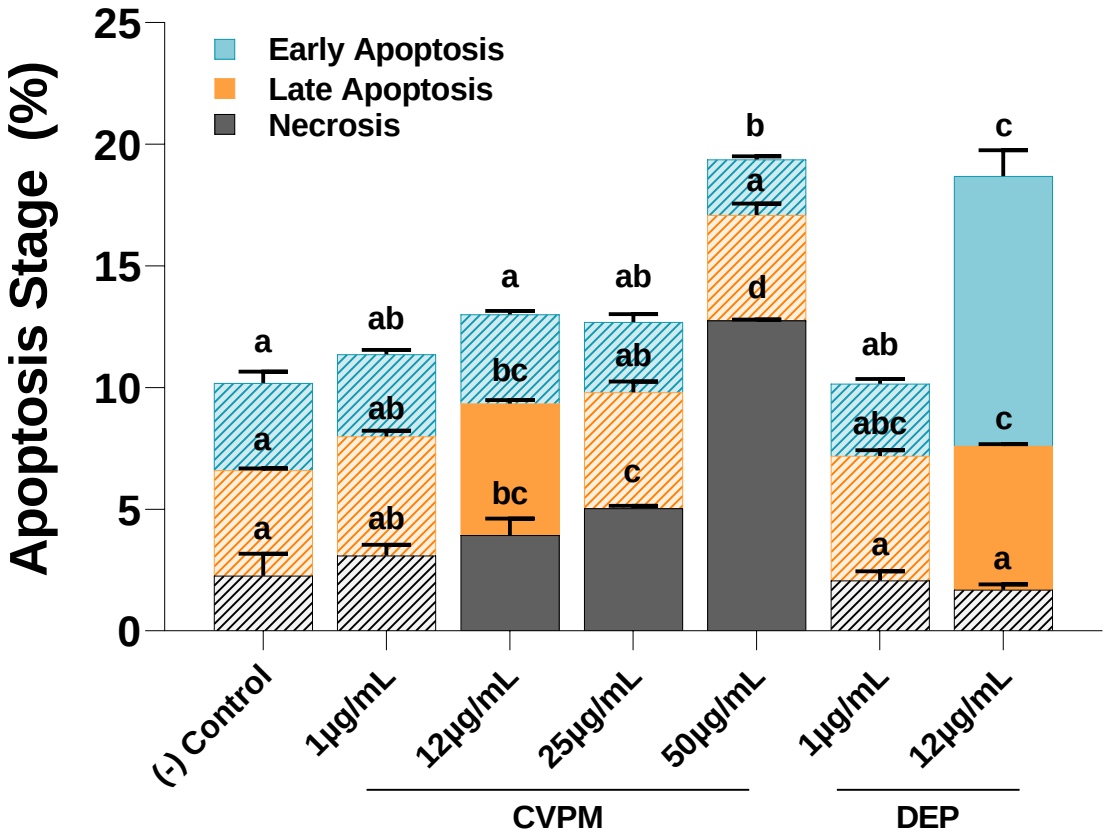

Figure 5.4. Apoptosis events at various stages (%; early apoptosis, late apoptosis, and necrosis) induced by CVPM and DEP following 24 hr exposures (N=3 per condition), where untreated samples were used as the negative control and 0.01% H_20_2 was used as the positive control (not shown). Bars with the same letter are not significantly different ($p \leq 0.05$ +/- 1 SD) and solid-colored bars indicate that the conditions are significant from the negative control. There appeared to be a concentration-related increase in necrotic cells corresponding to an increase in CVPM concentration and treatment with ≥12µg/mL CVPM was significant from both the negative control and equivalently tested concentrations of DEP. Exposure to 12µg/mL CVPM also caused a significant increase in cells in late-stage apoptosis compared to the negative control but there was no significant difference between CVPM and DEP at equivalent concentrations. At all tested concentrations, CVPM treatment did not cause a significant increase in early apoptosis events compared to the negative control and 12µg/mL DEP exposure resulted in a significant increase in cells in early apoptosis compared to 12µg/mL CVPM.

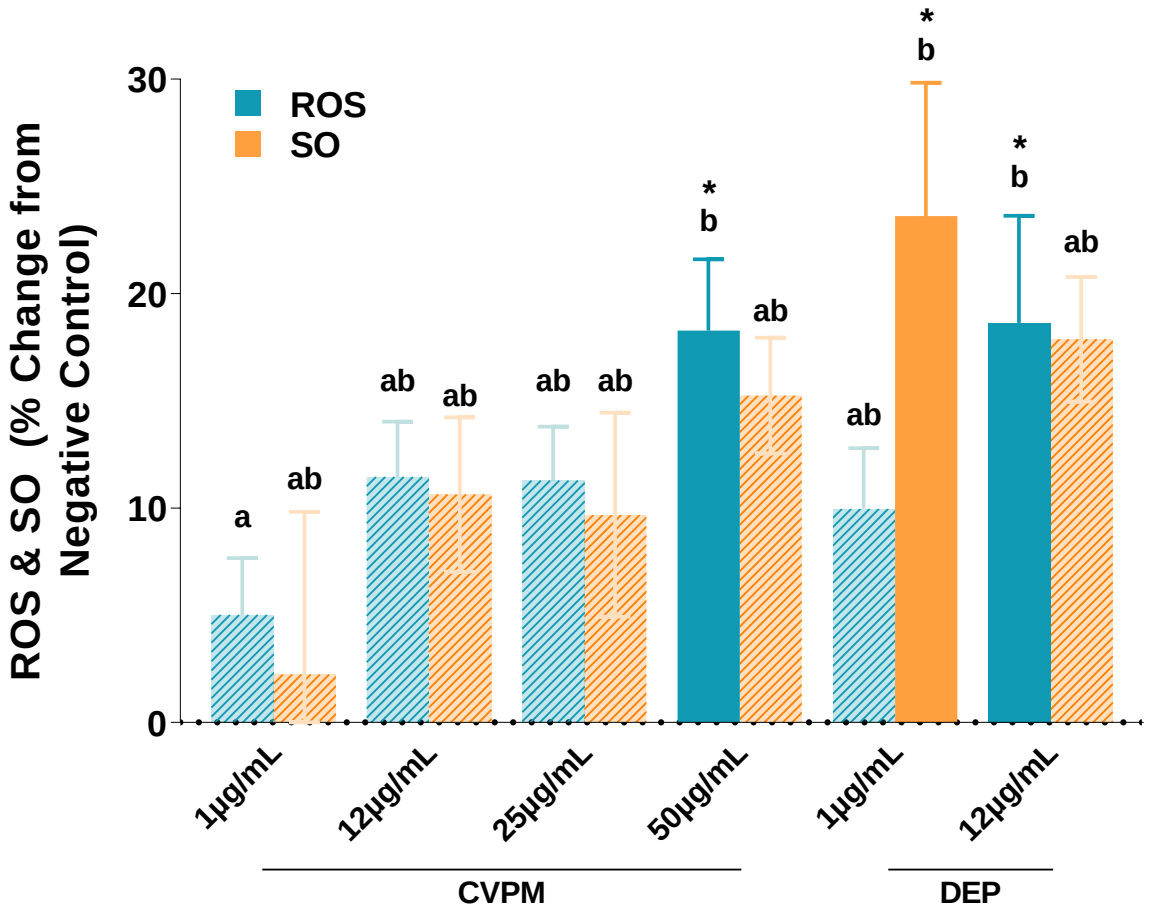

Figure 5.5. PM-induced oxidative stress as cellular ROS and SO following 24 hr exposure (% change from negative control; N=5 per condition), where pyocyanin (250µM) was used as the ROS positive control (not shown). Bars with the same letter are not significantly different and * with solid-colored bars indicate significant from the negative control ($p \leq 0.05$ +/- 1SD). There appeared to be a concentration-related increase in ROS production for CVPM and DEP, with 50µg/mL CVPM and 12µg/mL DEP being significantly increased compared to the negative control. Although not statistically significant, there also appeared to be a concentration-related increase in SO production for CVPM, but not DEP, and 1µg/mL DEP caused a significant increase in SO production compared to the negative control. While DEP exposure caused significant increases in both ROS and SO, in this assay there was no significant difference in ROS and SO production for equivalently tested CVPM and DEP concentrations.

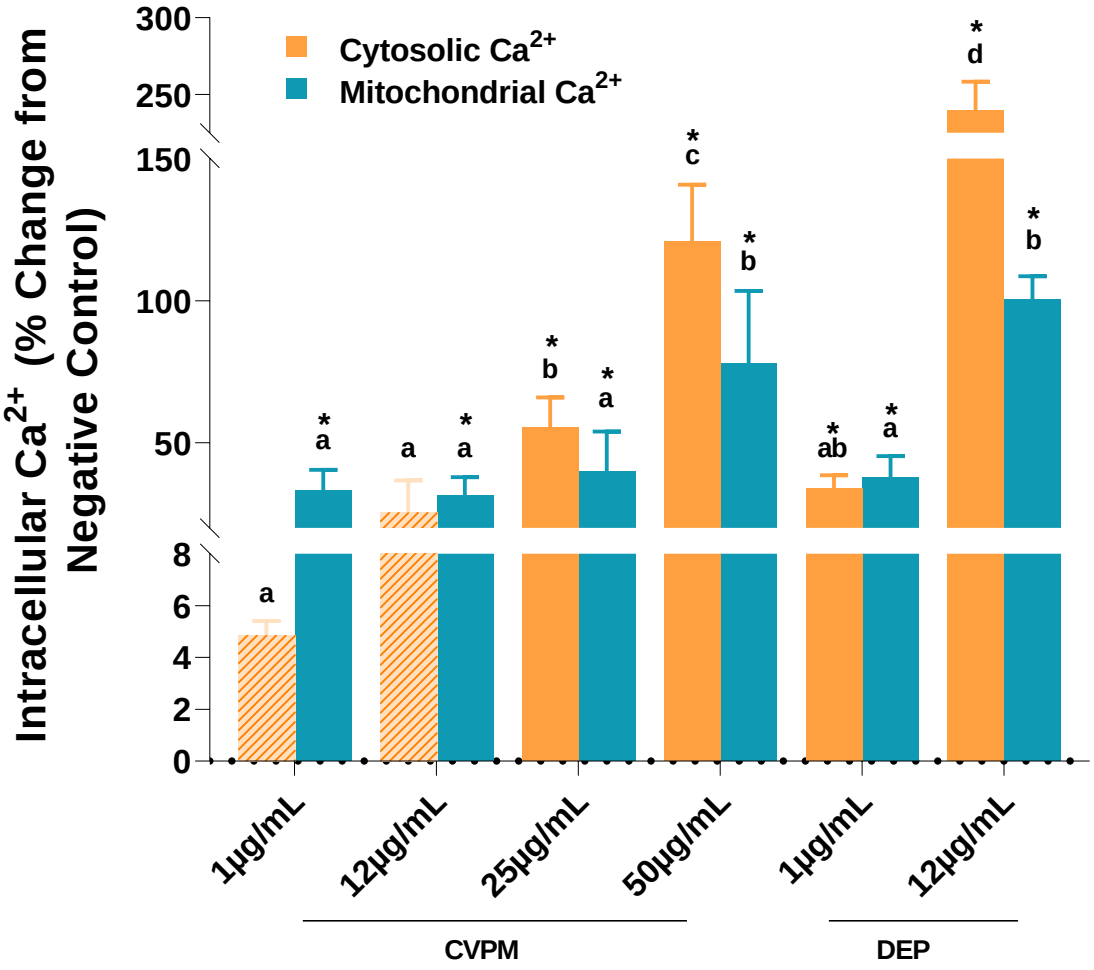

Figure 5.6. PM-induced cytosolic and mitochondrial Ca^{2+} flux following 24 hr exposure (% change from negative control; N=5 per condition). Bars with the same letter in each test group (i.e., cytosolic or mitochondria Ca^{2+}) are not significantly different and * with solid-colored bars indicate significant from the negative control (p=0.05 +/- 1 SD). There was a concentration-related increase in both cytosolic and mitochondrial Ca^{2+} concentrations in CVPM treated cells compared to the negative control. In both experiments, 12µg/mL DEP caused a significant increase in Ca^{2+} concentrations compared to 12µg/mL CVPM, suggesting DEP exposure overall more readily causes alterations in cellular Ca^{2+} homeostasis compared to CVPM.

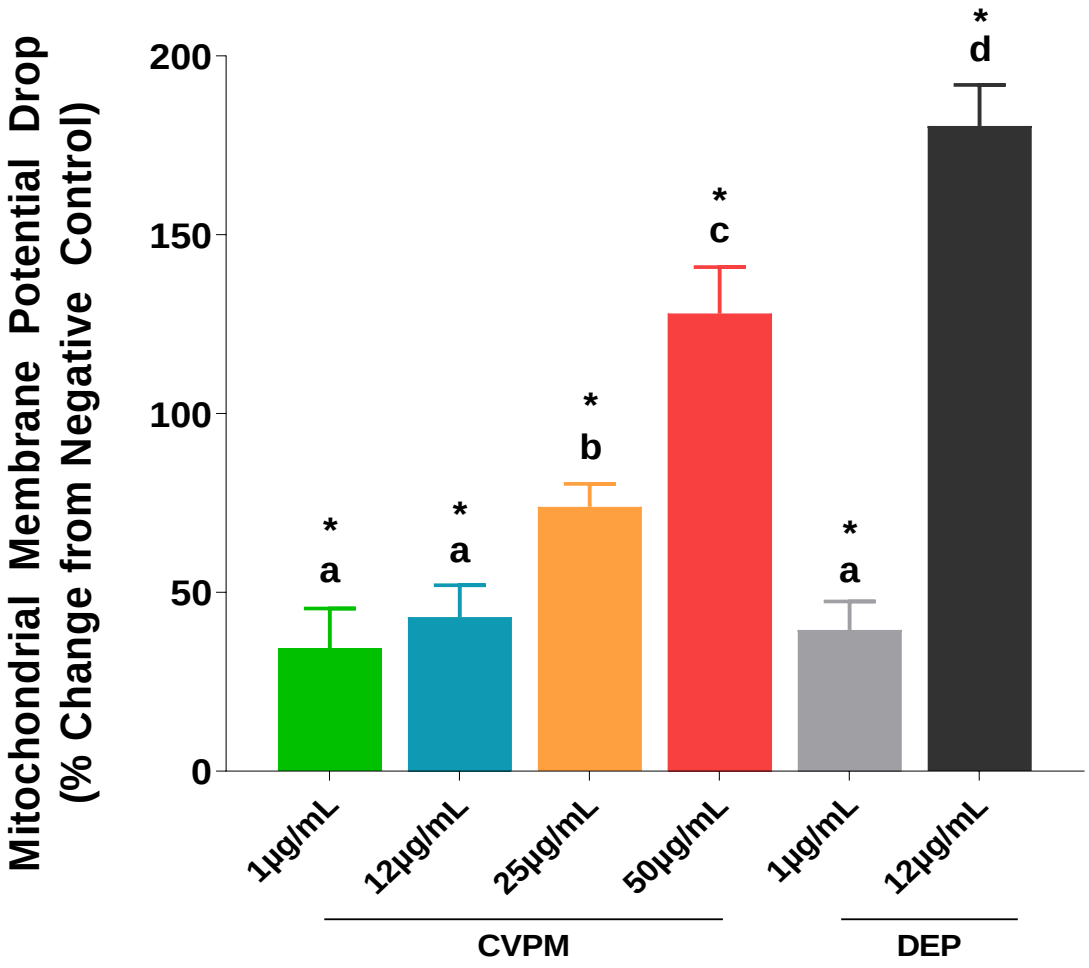

Figure 5.7. CVPM causes mitochondrial membrane potential (Δψm) depolarization at all tested concentrations (% change from negative control; N=5 per condition). CCCP (50µM), a chemical inhibitor of oxidative phosphorylation, was used as the positive control (not shown). Bars with the same letter are not significantly different and * = significant from the negative control ($p \leq 0.05$ +/- 1SD). There was a significant concentration-related decrease in Δψm for all CVPM treated conditions. Treatment with 12µg/mL DEP caused a significant drop in Δψm compared to 12µg/mL CVPM, but there was no significant difference in Δψm between 1µg/mL DEP and 1µg/mL CVPM.

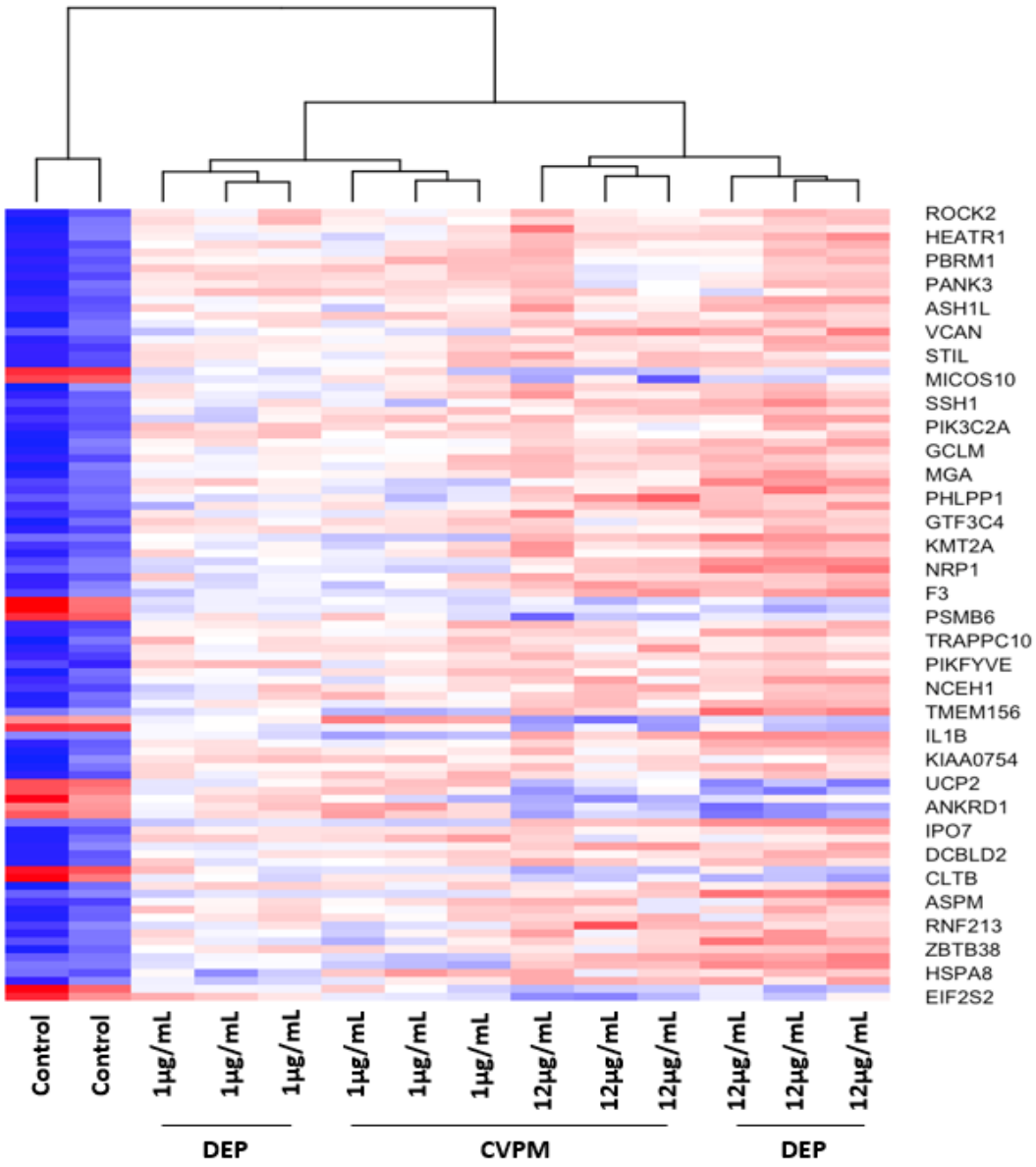

Figure 5.8. Heatmap of log counts per million (logCPM) values for the top 100 differentially expressed genes (DEGs) following CVPM and DEP treatment. Expression across each gene (i.e., row) have been scaled so that X expression = 0, S.D. = 1 (up expression in red, down expression blue). Lighter shades represent genes with intermediate expression levels. Samples and genes have been ordered by the method of hierarchical clustering and dendrogram at top represents sample clustering. Overall, individual samples clustered closest to their corresponding sample group, suggesting good replication was achieved. 12µg/mL CVPM clustered closest to 12µg/mL DEP and 1µg/mL CVPM clustered closest to 1µg/mL DEP. 12µg/mL DEP was least similar to the negative control, with more significantly upregulated and downregulated genes (i.e., darker opposite shades of blue and red).

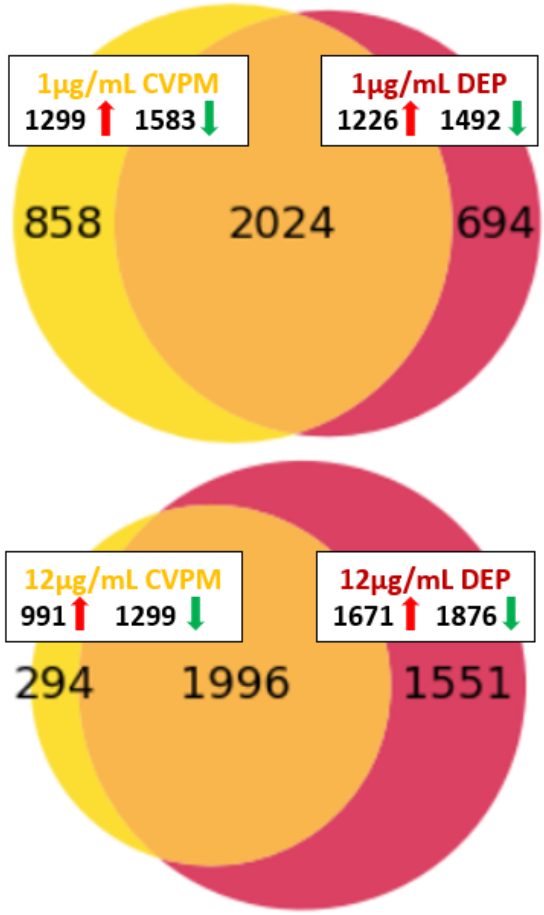

Figure 5.9. Distribution and direction of change of differentially expressed genes (DEGs) in BEAS-2B cells following CVPM and DEP exposure. For each comparison between particle types of the same concentration, the number of shared or unique DEGs are indicated (FDR = 0.05). Circle area is proportional to the number

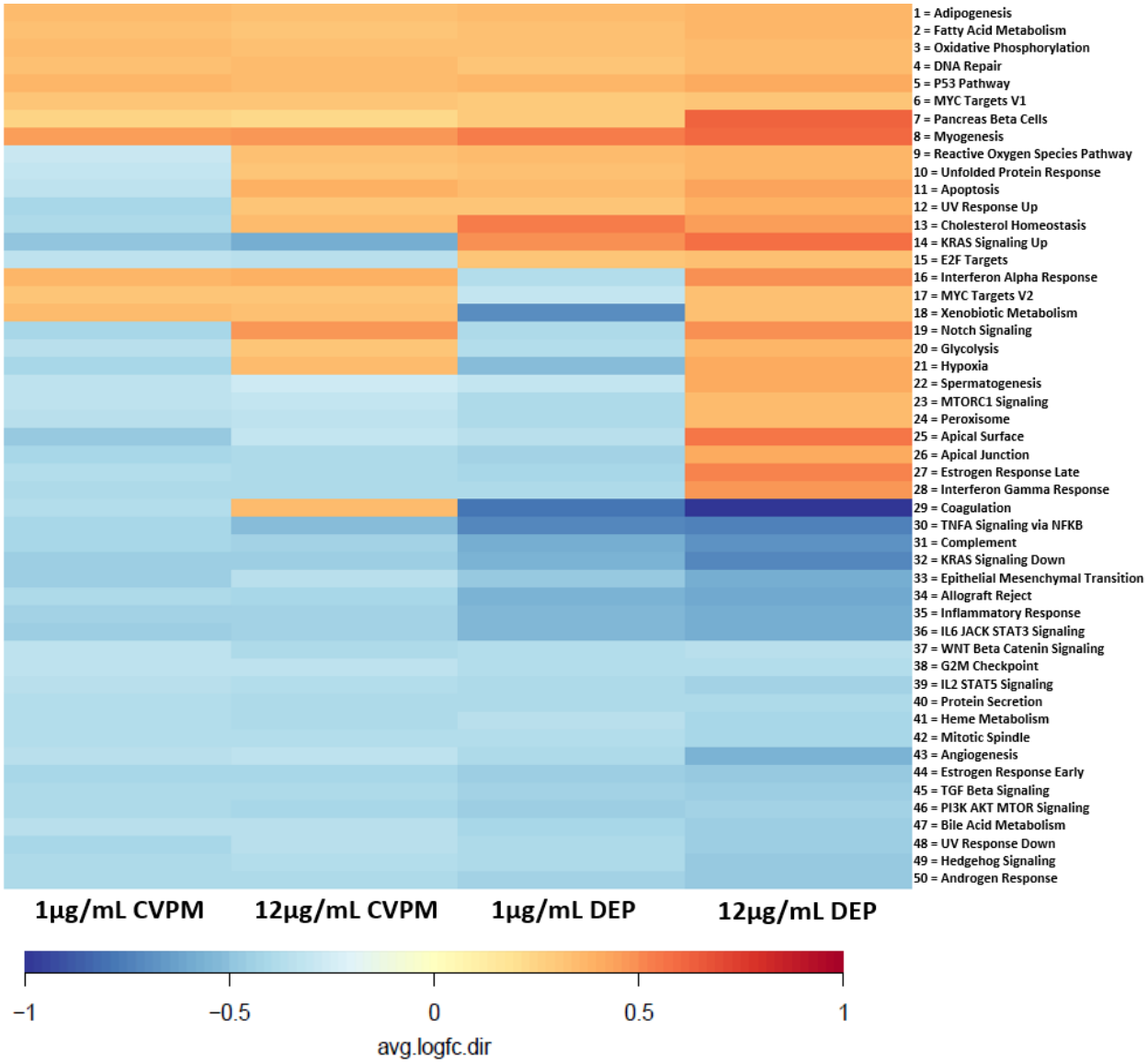

Figure 5.10. EGSEA summary heatmap of the top 50 significantly affected pathways (FDR = 0.05) following 24 hr CVPM and DEP exposure. The orange shades indicate the majority of the genes in the pathway are upregulated (i.e., have a positive average log fold change direction) and the blue shades indicate the majority of the genes in the pathway are downregulated (i.e., have a negative average log fold change direction). The majority of the known genes in the hallmark UPR pathway from MSigDB were significantly upregulated for 12µg/mL CVPM but downregulated for 1µg/mL CVPM. DEP exposure caused a more significant upregulation in the UPR pathway compared to CVPM at equivalently tested concentrations (FDR=0.05; p=0.007 for 12µg/mL CVPM, p=0.0001 for 12µg/mL DEP). Other affected biological pathways of interest related to the UPR include apoptosis, ROS, and the inflammatory response.

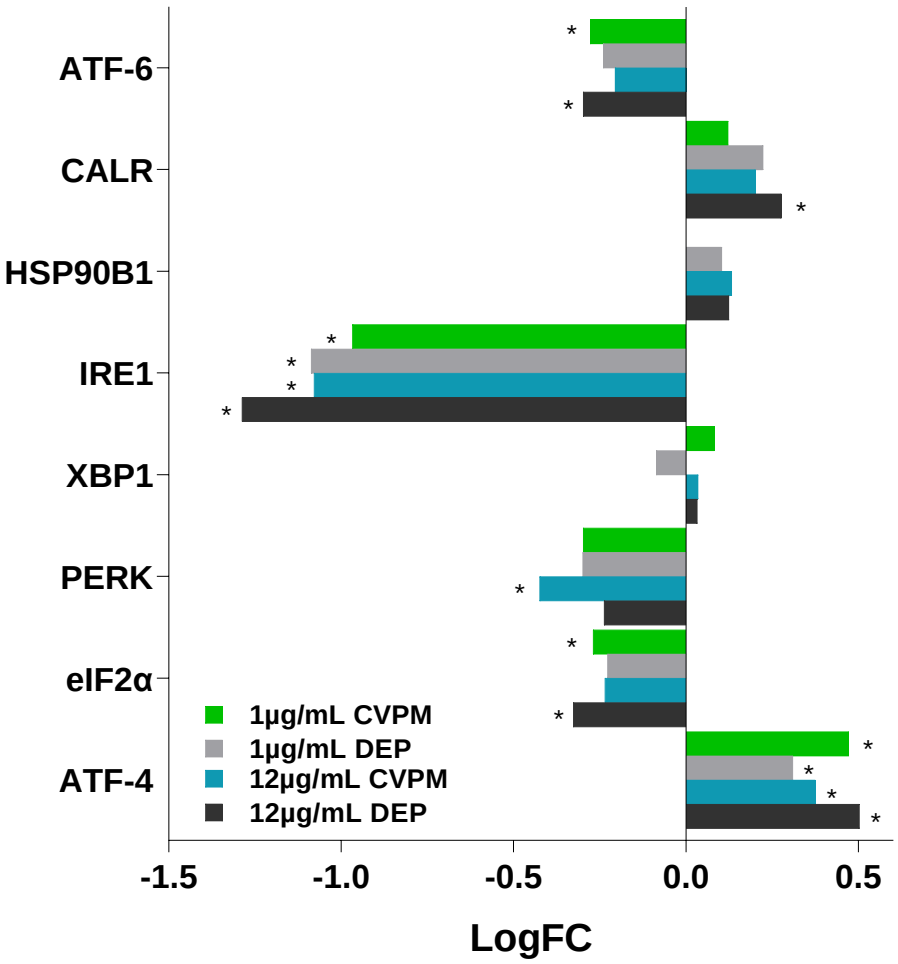

Figure 5.11. Expression of UPR pathway genes of interest in BEAS-2B cells after 24 hr treatment with CVPM and DEP as log fold change (logFC) direction results (* = significant from the negative control; FDR=0.05). CVPM exposure caused an overall downregulation of the three primary UPR transducer genes: activating transcription factor 6 (ATF-6), inositol-requiring enzyme 1 (IRE1), and pancreatic PRK-like ER kinase (PERK). At 1µg/mL, CVPM exposure caused a more significant downregulation for only ATF-6, while DEP exposure elicited a more significant downregulation for IRE1, and both particle types incited a similar response for PERK. At 12µg/mL, CVPM exposure caused a more significant downregulation for only PERK, while DEP exposure caused a more significant downregulation for both ATF-6 and IRE1. CVPM treatment at all tested concentrations caused an upregulation of the ER chaperone calreticulin (CALR), while only 12µg/mL CVPM caused an upregulation of the ER chaperone glucose-regulated protein 94 (HSP90B1/ GRP94), downstream effectors of ATF-6 activation. At equivalently tested concentrations, DEP exposure caused more upregulation of both HSP90B1 and CALR, however, only 12µg/mL DEP for CALR was significant. Although not significant, a major downstream effector of the UPR transducer protein IRE1, x-box binding protein 1 (XBP1), was upregulated across all tested CVPM concentrations. At 1µg/mL, DEP exposure caused a downregulation of XBP1 compared to CVPM and 12µg/mL CVPM and DEP exposure induced similar logFC changes in XBP1 expression. CVPM exposure also caused a significant downregulation of eukaryotic initiation factor-2α (eIF2α) and significant upregulation of activating transcription factor 4 (ATF-4), important downstream targets of PERK activation. Exposure to 1µg/mL CVPM elicited a more significant change in eIF2α and ATF-4 compared to 1µg/mL DEP. However, 12µg/mL DEP caused a more significant response in both eIF2α and ATF-4 compared to 12µg/mL CVPM.

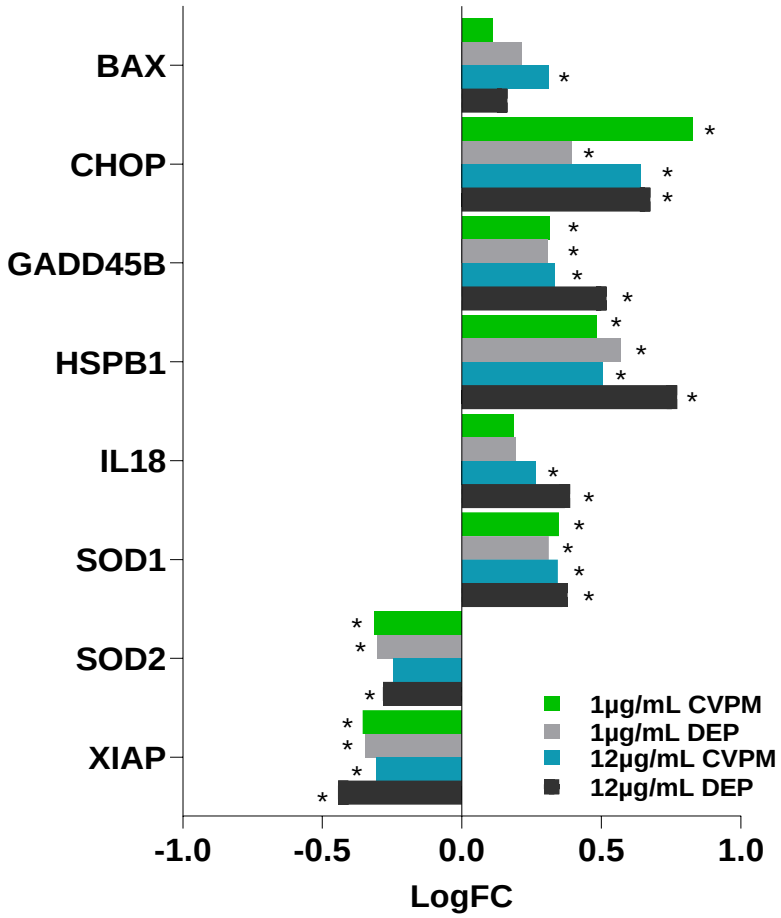

Figure 5.12. Expression of apoptosis pathway genes of interest in BEAS-2B cells after 24 hr treatment with CVPM and DEP as log fold change (logFC) direction results (* = significant from the negative control; FDR=0.05). CVPM treatment elicited an upregulation in BCL2 associated X apoptosis regulator (BAX), a pro-apoptotic member of the BL2-family that facilitates apoptotic signaling events, C/EBP homologous protein (CHOP), an important component of UPR-related apoptosis via the PERK-ATF4-CHOP pathway, heat shock protein B1 (HSPB1/HSP27), growth arrest and DNA damage inducible beta (GADD45B), a CHOP-induced blocking agent of protein synthesis, and the pro-inflammatory cytokine interleukin-18 (IL18). At 1µg/mL treatment, CVPM caused a more significant upregulation in CHOP (p=0.005 for CVPM, p=0.02 for DEP), and DEP caused more significant upregulation in HSPB1 (p=0.01 for CVPM, p=0.005 for DEP), while GADD45B and IL-18 had similar expression levels (p=0.05 for CVPM, p=0.05 for DEP). At 12µg/mL, CVPM caused a more significant upregulation in BAX only (p=0.02 for CVPM, p=0.18 for DEP) and DEP caused more significant upregulation in CHOP (p=0.001 for CVPM, p=0.0005 for DEP), GADD45B (p=0.04 for CVPM, p=0.003 for DEP), HSPB1 (p=0.01 for CVPM, p=0.0005 for DEP), and IL-18 (p=0.02 for CVPM, p=0.002 for DEP). Superoxide dismutase 1 (SOD1) and superoxide dismutase 2 (SOD2) are primarily anti-apoptotic genes that function as ROS scavengers in the cytosol and mitochondria, respectively. Although CVPM treatment caused SOD1 upregulation, SOD2 was downregulated, which could contribute to mitochondrial stress leading to cytochrome c release and apoptosis. CVPM treatment at all tested concentrations also caused a downregulation of X-linked inhibitor of apoptosis (XIAP), an important intrinsic inhibitor of apoptosis, thus inducing apoptosis. At 1µg/mL, CVPM caused a more significant upregulation and downregulation in SOD1 (p=0.01 for CVPM, p=0.02 for DEP) and XIAP (p=0.003 for CVPM, p=0.005 for DEP) compared to DEP, while SOD2 had similar expression levels (p=0.02 for CVPM, p=0.02 for DEP). At 12µg/mL, DEP caused more significant upregulation in SOD1 (p=0.01 for CVPM, p=0.004 for DEP), and downregulation in SOD2 (p=0.06 for CVPM, p=0.02 for DEP) and XIAP (p=0.009 for CVPM, p=0.005 for DEP) compared to CVPM.

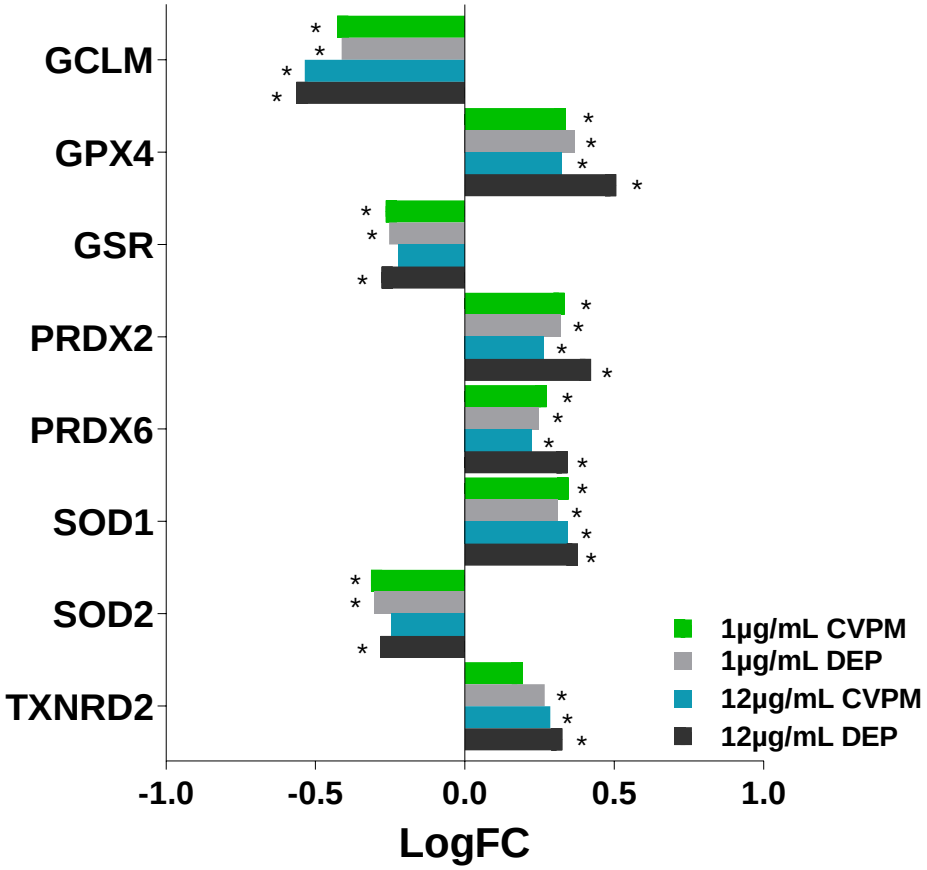

Figure 5.13. Expression of ROS pathway genes of interest in BEAS-2B cells after 24 hr treatment with CVPM and DEP as log fold change (logFC) direction results (* = significant from the negative control; FDR=0.05). Across all CVPM-treated conditions, glutamate-cysteine ligase regulatory subunit (GCLM), a protein-encoding gene involved in synthesis of glutathione which functions as a main antioxidant against ROS, glutathione reductase (GSR), which encodes an enzyme that is responsible for maintaining the supply of reduced (i.e., active form) of glutathione, and superoxide dismutase 2 (SOD2), a scavenger of ROS byproducts of oxidative phosphorylation, were downregulated thus indicating that the cell is likely more susceptible to the effects oxidative stress, including activation of the UPR and the inflammatory response. At 1µg/mL, CVPM caused a more significant downregulation of GLCM compared to DEP (p=0.001 for CVPM, p=0.002 for DEP), while GSR (p=0.03 for CVPM, p=0.03 for DEP) and SOD2 (p=0.02 for CVPM, p=0.02 for DEP) had similar expressions. At 12µg/mL, DEP caused a more significant downregulation of GCLM (p=0.004 for CVPM, p=0.0001 for DEP), GSR (p=0.07 for CVPM, p=0.02 for DEP), and SOD2 (p=0.06 for CVPM, p=0.02 for DEP) compared to CVPM. In addition, CVPM exposure caused an upregulation of glutathione peroxidase 4 (GPX4), peroxiredoxin-2 (PRDX2), peroxiredoxin-6 (PRDX6), superoxide dismutase 1 (SOD1), and thioredoxin reductase 2 (TXNRD2), which function by reducing or eliminating ROS to protect the cell from oxidative stress, indicating the cell is responding to oxidative insult. At 1µg/mL, CVPM exposure caused a more significant upregulation of PRDX6 (p=0.009 for CVPM, p=0.01 for DEP) and SOD1 (p=0.01 for CVPM, p=0.02 for DEP), while DEP caused a more significant upregulation of GPX4 (p=0.02 for CVPM, p=0.01 for DEP) and TXNRD2 (p=0.09 for CVPM, p=0.02 for DEP), with similar expression for PRDX2 (p=0.01 for CVPM, p=0.01 for DEP). At 12µg/mL, DEP caused a more significant upregulation of GPX4 (p=0.03 for CVPM, p=0.001 for DEP), PRDX2 (p=0.03 for CVPM, p=0.001 for DEP), PRDX6 (p=0.02 for CVPM, p=0.001 for DEP), SOD1 (p=0.01 for CVPM, p=0.004 for DEP) and TXNRD2 (p=0.02 for CVPM, p=0.007 for DEP).

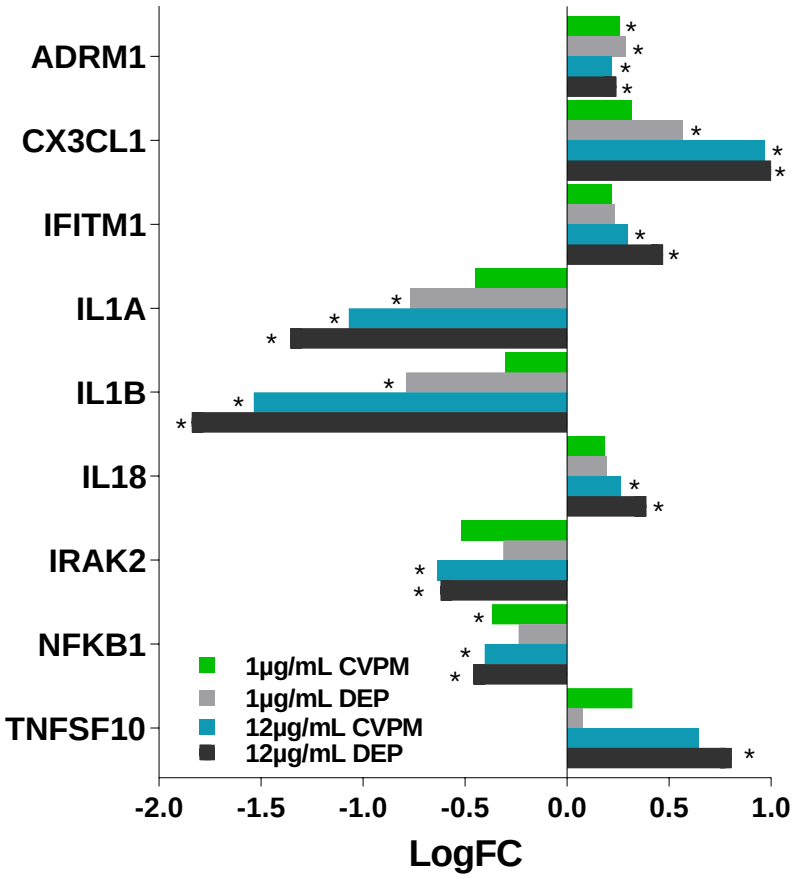

Figure 5.14. Expression of inflammatory response pathway genes of interest in BEAS-2B cells after 24 hr treatment with CVPM and DEP as log fold change (logFC) direction results (* = significant from the negative control; FDR=0.05). For all tested concentrations of CVPM, interleukin-1α (IL1A), interleukin-1β (IL1B), interleukin-1 receptor-associated kinase 2 (IRAK2), nuclear factor-kappa B (NFKB1) were downregulated across all conditions, indicating attenuation of several primary inflammatory response mediators. At 1µg/mL, CVPM exposure caused a more significant downregulation of NFKB1 (p=0.03 for CVPM, p=0.15 for DEP), while DEP caused a more significant downregulation of IL1A (p=0.13 for CVPM, p=0.015 for DEP) and IL1B (p=0.14 for CVPM, p=0.002 for DEP). At 12µg/mL, DEP exposure caused a more significant downregulation for IL1A (p=0.002 for CVPM, p=0.0003 for DEP), IL1B (p=0.000003 for CVPM, p=0.0000001 for DEP), IRAK2 (p=0.05 for CVPM, p=0.04 for DEP), and NFKB1(p=0.02 for CVPM, p=0.007 for DEP). In addition, fractalkine/chemokine (C-X3-C motif) ligand 1 (CX3CL1), interferon-induced transmembrane protein 1 (IFITM1), interleukin-18 (IL18), tumor necrosis factor superfamily member 10 (TNFSF10), proinflammatory cytokines related to apoptosis, and proteasomal ubiquitin receptor (ADRM1), which plays a key role in homeostasis by assisting the removal of misfolded or damaged proteins, were upregulated across all CVPM test conditions suggesting that CVPM exposure activated members of the inflammatory response pathway related to UPR initiation. At 1µg/mL, DEP caused a more significant upregulation of ADRM1 (p=0.02 for CVPM, p=0.01 for DEP) and CX3CL1 (p=0.22 for CVPM, p=0.04 for DEP). At 12µg/mL, DEP caused a more significant upregulation of ADRM1 (p=0.04 for CVPM, p=0.02 for DEP), CX3CL1 (p=0.004 for CVPM, p=0.001 for DEP), IFITM1 (p=0.04 for CVPM, p=0.002 for DEP), IL18 (p=0.03 for CVPM, p=0.002 for DEP), and TNFSF10 (p=0.11 for CVPM, p=0.04 for DEP) compared to CVPM.

6.0. REFERENCES

Alhamdoosh M., Law C. W., Tian L., Sheridan J. M., Ng M., Ritchie M. E. (2017). Easy and efficient ensemble gene set testing with EGSEA. *F1000Research*. **6**(2010):1-38.

Alirol E., James D., Huber D., Marchetto A., Vergani L., Martinou J. C., Scorrano L. (2006). The mitochondrial fission protein hFis I requires the endoplasmic reticulum gateway to induce apoptosis. *Molecular Biology of the Cell*. **17**:4593-4605.

Archer V. E. (1990). Air Pollution and Fatal Lung Disease in Three Utah Counties. *Archives of Environmental Health*. **45**(6):325-334.

Baasandorj M., Brown S., Hoch S., Crosman E., Long R., Silva P., Mitchell L., Hammond I., Martin R., Bares R., Lin J., Sohl J., Page J., McKeen S., Pennell C., Franchin A., Middlebrook A., Peterson R., Hallar G., Fibiger D., Womack C., McDuffie E., Moravek A., Murphy J., Hrdina A., Thorton J., Goldberger L., Lee B., Riedel T., Whitehill A., Kelly K., Hansen J., Eatough D. (2018). 2017 Utah Winter Fine Particulate Study Final Report.

B'chir W., Maurin A-C., Carraro V., Averous J., Jousse C., Muranishi Y., Parry L., Stepien G., Fafournoux., Bruhat A. (2013). The eIF2α/ATF4 pathway is essential for stress-induced autophagy gene expression. *Nucleic Acids Research*. **41**(16): 7683-7699.

Becker S., Dailey L., Soukup J., Grambow S., Devlin R., Huang Y.-C. (2005). Seasonal Variations in Air Pollution Particle-Induced Inflammatory Mediator Release and Oxidative Stress. *Environmental Health Perspectives*. **113**(8):1032-1038.

Becker S., Mundandhara S., Devlin R. B., Madden M. (2005). Regulation of cytokine production in human alveolar macrophages and airway epithelial cells in response to ambient air pollution particles: further mechanistic studies. *Toxicology and Applied Pharmacology*. **208**:269-275.

Bettigole S. E., Glimcher L. H. (2015). Endoplasmic Reticulum Stress and Immunity. *Annual Review of Immunology*. **33**:107-138.

Bhat T A., Chaudhary A. K., Kumar S., O'Malley J., Inigo J. R., Kumar R., Yadav N., Chandra D. (2017). Endoplasmic reticulum-mediated unfolded protein response and mitochondrial apoptosis in cancer. *Biochimica et Biophysica Acta*. **1867**:58-66.

Bobrovnikova-Marjon E., Grigoriadou C., Pytel D., Zhang F., Ye J., Koumenis C., Cavener D., Diehl J. A. (2010). PERK promotes cancer cell proliferation and tumor growth by limiting oxidative DNA damage. *Oncogene*. **29**(27)3881-3895.

Bowe B., Xie Y., Yan Y., Al-Aly Z. (2019). Burden of Cause-Specific Mortality Associated with $PM_{2.5}$ Air Pollution in the United States. *JAMA Network Open*. **2**(11): 1-16.

Bravo R., Vicencio J. M., Parra v., Troncoso R., Munoz J. P., Bui M., Quiroga C., Rodriguez A. E., Verdejo H. E., Ferreira J., Iglewski M., Chiong M., Simmen T., Zorzano A., Hill J. A., Rothermel B. A., Szabadkai G., Lavandero S. (2011). Increased ER-mitochondrial coupling promotes mitochondrial respiration and bioenergetic during early phases of ER stress. *Journal of Cell Science*. **124**(14):2143-2152.

Brown, D. M., Donaldson, K., and Stone, V. (2004). Effects of PM_{10} in human peripheral blood monocytes and J774 macrophages. *Respiratory Research*. **5**:29

Brown, D. M., Hutchison, L., Donaldson, K., and Stone, V. (2007). The effects of PM_{10} particles and oxidative stress on macrophages and lung epithelial cells: Modulating effects of calcium signaling antagonists. *American Journal of Physiology - Lung Cellular and Molecular Physiology*. **292**: L1444–L1451.

Brunekreef B., Holgate S. (2002). Air pollution and health. *The Lancet*. **360**(9341): 1233-1242.

Calderon-Garciduenas L., Leray E., Heydarpour P., Torres-Jardon R., Reis J. (2016). Air pollution, a rising environmental risk factor for cognition, neuroinflammation and neurodegeneration: The clinical impact on children and beyond. *Revue Neurologique*. **172**:69-80.

Chaudhari N., Talwar P., Parimisetty A., d'Hellencourt L., Ravanan P. (2014). A molecular web: endoplasmic reticulum stress, inflammation, and oxidative stress. *Frontiers in Cellular Neuroscience*. **8**(213):1-15.

Chen H., Burnette R. T., Kwong J. C., Villeneuve P. J., Goldberg M. S., Brook R. D., Donkelaar A., Jerrett M., Martin R. V., Brook J. R., Copes R. (2013). Risk of Incident Diabetes in Relation to Long-term Exposure to Fine Particulate Matter in Ontario, Canada. *Environmental Health Perspectives*. **121**(7):804-810.

Chen L., Deng H., Cui H., Fang J., Zuo Z., Deng J., Li Y., Wang X., Zhao L. (2018). Inflammatory responses and inflammation-associated diseases in organs. *Oncotarget*. **9**(6):7204-7218.

Coleman N. C., Burnett R. T., Higbee J. D., Lefler J. S., Merrill R. M., Ezzati M., Marshall J. D., Kim S., Bechle M., Robinson A. L., Pope III C. A. (2020). Cancer mortality risk fine particulate air pollution, and smoking in a large, representative cohort of US adults. *Cancer Causes & Control*. **31**:767-776.

Cooks T., Harris C. Oren M. (2014). Caught in the crossfire: p53 in inflammation. *Carcinogenesis*. **35**(8):1680-1690.

Dockery et al., (1993). An Association between Air Pollution and Mortality in Six U.S. Cities. *The New England Journal of Medicine*. **329**(24):1753-1759.

Dockery D. W., Pope III C. A. (1994). Acute Respiratory Effects of Particulate Air Pollution. *Annual Reviews of Public Health*. **15**:107-132.

Environmental Protection Agency (2021). Retrieved from https://www.epa.gov/pm-pollution/timeline-particulate-matter-pm-national-ambient-air-quality-standards-naaqs

Fairley, D. (1990). The Relationship of Daily Mortality to Suspended Particulates in Santa Clara County, 1980-1986. *Environmental Health Perspectives*. **89**:159-168.

Gillies. R. R., Wang S.-Y., Booth M. R. (2010). Atmospheric scale interaction on wintertime Intermountain West low-level inversions. *Weather Forecasting*. **25**:1196-1210.

Greenbaum D., Colangelo C., Williams K., Gerstein M. (2003). Comparing protein abundance and mRNA expression levels on a genomic scale. *Genome Biology*. **4**(117):1-8.

Grootjans J., Kaser A., Kaufman R. J. (2016). The unfolded protein response in immunity and inflammation. *Nature Reviews Immunology*. **16**:469-484

Gurzov E. N., Ortis F., Bakiri L., Wagner E. F., Eizirik D. L., (2008). JunB inhibits ER stress and apoptosis in pancreatic beta cells. *PLoS ONE*. **3**:e3030.

Gurzov E. N., Ortis F., Cunha D. A., Gosset G., Li M., Cardozo A. K., Eizirik D. L., (2009). Signaling by IL-1betta + IFN-gamma and ER stress converge on DP5/Hrk activation: A novel mechanism for pancreatic beta-cell apoptosis. *Cell Death Differ*. **16**:1539-1550.

Gurzov E. N., Germano C. M., Cunha D. A., Ortis F., Vanderwinden J. M., Marchetti P., Zhang L., Eizirik D. L., (2010). P53 up-regulated modulator of apoptosis (PUMA) activation contributes to pancreatic beta-cell apoptosis induced by proinflammatory cytokines and endoplasmic reticulum stress. *Journal of Biological Chemistry*. **285**:19910-19920.

Haeri M., Knox B E. (2012). Endoplasmic Reticulum Stress and Unfolded Protein Response Pathways: Potential for Treating Age-related Retinal Degeneration. *Journal of Ophthalmic and Vision Research*. **7**(1):45-57.

Hanai A., Antkiewicz D. S., Hemming J., Shafer M., Lai A., Arhami M., Hosseini V., Schauer J. J. (2019). Seasonal variations in the oxidative stress and inflammatory potential of $PM_{2.5}$ in Tehran using an alveolar macrophage model; The role of chemical composition and sources. *Environmental International*. **123**:417-427.

Harding H., Ron D. (2002). Endoplasmic Reticulum Stress and the Development of Diabetes. *Diabetes*. **51**:455-461.

Hetz C. (2012). The unfolded protein response: controlling cell fate decisions under ER stress and beyond. *Nature Reviews*. **13**:89-102.

Hotamisligil G. S. (2010). Endoplasmic Reticulum Stress and the Inflammatory Basis of Metabolic Disease. *Cell*. **140**(6): 900-917.

Hu H., Tian M., Ding C., Yu S. (2019). The C/EBP Homologous Protein (CHOP) Transcription Factor Functions in Endoplasmic Reticulum Stress-Induced Apoptosis and Microbial Infection. *Frontiers in Immunology*. **9**(3083):1-13.

International Agency for Research on Cancer (2013). Air Pollution and Cancer. Retrieved from https://publications.iarc.fr/Book-And-Report-Series/Iarc-Scientific-Publications/Air-Pollution-And-Cancer-2013

Jamora C., Dennert G., Lee A. S. (1996). Inhibition of tumor progression by suppression of stress protein GRP78/BiP induction in fibrosarcoma B/C10ME. *PNAS*. **93**(15):7690-7694.

Jung C., Lin Y., Hwang B. (2015). Ozone, particulate matter, and newly diagnosed Alzheimer's disease: a population-based cohort study in Taiwan. *Journal of Alzheimer's Disease*. **44**(2):573-584.

Kadowaki H., Nishitoh H. (2013). Signaling Pathways form the Endoplasmic Reticulum and Their Roles in Disease. *Genes*. **4**(3):306-333.

Kawanishi S., Ohnishi S., Ma N., Hiraku Y., Murata M. (2017). Crosstalk between DNA Damage and Inflammation in the Multiple Steps of Carcinogenesis. *International Journal of Molecular Sciences*. **18**:1-13.

Kim D., Langmead B., Salzber S. L. (2015). HISAT: a fast spliced aligner with low memory requirements. *Nature Methods*. **12**(4):357-360.

Kozutsumi Y., Segal M., Normington K., Gething M. J., Sambrook J. (1988). The presence of malfolded proteins in the endoplasmic reticulum signals the induction of glucose-regulated proteins. *Nature*. **332**:462-464.

Kudo T., Katayama T., Imaizumi K., Yasuda Y., Yatera M., Okochi M., Tohyama M., Takeda M., (2002). The unfolded protein response is involved in the pathology of Alzheimer's disease. *Annual NY Academy of Science*. **977**:349-355.

Laing S., Wang G., Briazova T., Zhang C., Wang A., Zheng Z., Gow A., Chen A. F., Rajagopalan S., Chen L. C., Sun Q., Zhang K. (2010). Airborne particulate matter selectively activates endoplasmic reticulum stress response in the lung and liver tissues. *American Journal of Physiology-Cell Physiology*. **299**:736–749.

Law C. W., Alhamdoosh M., Su S., Dong X., Tian L., Smyth G. K., Ritchie M. E. (2018). RNA-seq analysis is easy as 1-2-3 with limma, Glimma and edgeR. *F1000Research*. **5**(1408):1-29.

Lecercq B., Kluza J., Antherieu S., Sotty J., Alleman L.-Y., Perdrix E., Loyens A., Coddeville P., Lo Guidice J.-M., Marchetti P., Garcon G. (2018). Air pollution derived $PM_{2.5}$ impairs mitochondrial function in healthy and chronic obstructive pulmonary diseased human bronchial epithelial cells. *Environmental Pollution*. **243**:434-1449.

Leung L. R., Gustafson Jr. W. I. (2005). Potential regional climate change and implications to U.S. air quality. *Geophysical Research Letters*. **32**(6):1-4.

Li Y., Guo Y., Tang J., Jiang J., Chen Z. (2014). New insights into the roles of CHOP-induced apoptosis in ER stress. *Acta Biochimica et Biophysica Sinica*. **46**:629-640.

Li Y., Duan J., Yang M., Li Y., Jing L., Yu Y., Wang J., Sun Z. (2017). Transcriptomic analyses of human bronchial epithelial cells BEAS-2B exposed to atmospheric fine particulate $PM_{2.5.}$ *Toxicology in Vitro*. **42**:171-181.

Liao Y., Smyth G. K., Shi W. (2014). featureCounts: an efficient general-purpose program for assigning sequence reads to genomic features. *Bioinformatics*. **30**(7):923-930.

Liberzon A., Birger C., Thorvaldsdottir H., Ghandi M., Mesirov J. P., Tamayo P. (2015). The Molecular Signatures Database (MSigDB) hallmark gene set collection. *Cell Systems.* **1**(6):417-425.

Liu Y., Chen Y., Cao J., Tao F., Zhu X., Yao C., Chen D., Che Z., Zhao Q., Wen L. (2015). Oxidative stress, apoptosis, and cell cycle arrest are induced in primary fetal alveolar type II epithelial cells exposed to fine particulate matter from cooking oil fumes. *Environmental Science and Pollution Research*. **22**:9728-9741.

Liu X., Zhao Z., Li X., Lv S., Ma R., Qi Y., Abulikemu A., Duan H., Guo C., Li Y., Sun Z. (2020). $PM_{2.5}$ triggered apoptosis in lung epithelial cells through the mitochondrial

apoptotic way mediated by a ROS-DRP1-mitochondrial fission axis. *Journal of Hazardous Materials.* **390**(10):1-15.

Liu S., Wang Z., Jiang X., Gan J., Tian X., Xing Z., Yan Y., Chen J., Zhang J., Wang C., Dong L. (2021). Denatured corona proteins mediate the intracellular bioactivities of nanoparticles via the unfolded protein response. *Biomaterials*. **265**(2021):1-14.

Longhin, E., Holme, J.A., Gutzkow, K.B., Arlt, V.M., Kucab, J.E., Camatini, M., Gualtieri, M. (2013). Cell cycle alterations induced by urban $PM_{2.5}$ in bronchial epithelial cells: characterization of the process and possible mechanisms involved. *Particle and Fibre Toxicology*. **10**(63):1-19.

Longhin E., Holme J. A., Gualtieri M., Camatini M., Ovrevik J. (2018). Milan winter fine particulate matter ($wPM_{2.5}$) induces IL-6 and IL-8 synthesis in human bronchial BEAS-2B cells, but specifically impairs IL-8 release. *Toxicology in Vitro*. **52**:365-373.

Lurmann F.W., Brown S.G., McCarthy M.C., Roberts P.T. (2006). Processes influencing secondary aerosol formation in the San Joaquin Valley during winter. *Journal of the Air and Waste Management Association.* **56**(12):1679-1693.

Malek, E., Davis, T., Martin, R. S., and Silva P.J. (2006). Meteorological and environmental aspects of one of the worst national air pollution episodes (January, 2004) in Logan, Cache Valley, Utah, USA. *Atmospheric Research*. **79**:108-122.

Mangelson N., Lewis L., Joseph J., Cui W., Machir J., Eatough D. J., Rees L. B., Wilkerson T., Jensen D. T. (1997). The Contribution of Sulfate and Nitrate to Atmospheric Fine Particles During Winter Inversion Fogs in Cache Valley, Utah. *Journal of the Air & Waste Management Association*. **47**(2):167-175.

Marciniak S., Yun C., Oyadomari S., Novoa I., Zhang Y., Jungreis R., Nagata K., Harding H., Ron D. (2004). CHOP induces death by promoting protein synthesis and oxidation in the stressed endoplasmic reticulum. *Genes & Development*. **18**:3066-3077.

Martin R., Koford G. (2004). Ambient particulate matter ($PM_{2.5}$ and PM_{10}) in northern Utah's Cache Valley. Presented at the 97th Annual Conference and Exhibition of the Air and Waste Management Association, June 22-25, 2014. Paper 624.

Martin R. (2006). Cache Valley Air Quality Studies.

Martin, R. Coulombe, R.; and Brain, R., "Utah Air Quality: PM 2.5" (2016). All Current Publications. Paper 784.

Mendez R., Zheng Z., Fan Z., Rajagopalan S., Sun Q., Zhang K. (2013). Exposure to fine airborne particulate matter induces macrophage infiltration, unfolded proteins response, and lipid deposition in white adipose tissue. *America Journal of Translational Research*. **5**(2):224-234.

Mukerjee S., Smith L., Long R., Lonneman W., Kaushik S., Oliver K., Whitaker D. (2019). Particulate matter, nitrogen oxides, ozone, and select volatile organic compounds during a winter sampling period in Logan, Utah, USA. *Journal of the Air & Waste Management Association*. **69**(6):778-788.

Peters A., Veronesi B., Calderon-Garciduenas L., Gehr P., Chen L. C., Geiser M., Reed W., Rothen-Rutishauser B., Schurch S., Schulz H. (2006). Translocation and potential neurological effects of fine and ultrafine particles a critical update. *Particulate Fibre Toxicology*. **3**(13):1-13.

Pope III C. A., Schwartz J., Ransom M. R. (1992). Daily Mortality and PM_{10} Pollution in Utah Valley. *Archives of Environmental Health: An International Journal*. **47**(3):211-217.

Pope III C. A., Thun M. J., Namboodiri M. M., Dockery D. W., Evans J. S., Speizer F. E., Heath Jr. C W. (1995). Particulate air pollution as a predictor of mortality in a prospective study of U.S. adults. *American Journal of Respiratory and Critical Care Medicine*. **151**(3): 669-674.

Pope III C. A. (2000). Epidemiology of Fine Particulate Air Pollution and Human Health: Biologic Mechanisms and Who's at Risk? *Environmental Health Perspectives*. **108**(4):713-723.

Pope III C. A., Burnett, R.T., Thun, M.J., Calle, E.E., Krewski, D., Ito, K., Thurston, G.D. (2002). Lung cancer, cardiopulmonary mortality, and long-term exposure to fine particulate air pollution. *Journal of the Air & Waste Management Association*. **287**(9): 1132-1141.

Pope III C. A., Dockery, D.W. (2006). Health effects of fine particulate air pollution: Lines that connect. *Journal of the Air & Waste Management Association*. **56**(6):709-742.

Pope III C. A., Bhatnagar A., McCracken J. P., Abplanalp W., Conklin D. J., O'Toole T. (2016). Exposure to Fine Particular Air Pollution is Associated with Endothelial Injury and Systemic Inflammation. *Circulation Research*. **119**(11):1204-1214.

Read A., Schroder M. (2021). The Unfolded Protein Response: An Overview. *Biology*. **10**(384):1-10.

Rashid, H. O., Yadav, R. K., Kim, H. R., and Chae, H. J. (2015). ER stress: autophagy induction, inhibition and selection. *Autophagy*. **11**:1956–1977.

Rennard S.I., Basset G., Lecossier D., O'Donnell K.M., Pinkston P., Martin P.G. Crystal R.G. (1986). Estimation of volume of epithelial lining fluid recovered by lavage suing urea as marker of dilution. *Journal of Applied Physiology*. **60**:532-538.

Romero-Ramirez L., Cao H., Nelson D., Hammond E., Lee A.-H. Yoshida H., Mori K., Glimcher L. H., Denko N. C., Giaccia A. J., Le Q.-T., Koong A. C. (2004). XBP1 is essential for survival under hypoxic conditions and is required for tumor growth. *Cancer Research*. **64**:5943-5947.

Ron D., Walter P. (2007). Signal integration in the endoplasmic reticulum unfolded protein response. *Nature Reviews*. **8**:519-529.

Rozpedek W., Markiewica L., Diehl J. A., Pytel D., Majsterek I. (2015). Unfolded Protein Response and PERK Kinase as a New Therapeutic Target in the Pathogenesis of Alzheimer's Disease. *Current Medicinal Chemistry*. **22**(27):3169-3184.

Rutkowski D., Arnold S., Miller C., Wu J., Li J., Gunnison K., Mori K., Akha A., Raden D., Kaufman R. (2006). Adaptation to ER Stress Is Mediated by Differential Stabilities of Pro-Survival and Pro-Apoptotic mRNAs and Proteins. *PLoS Biology*. **4**(11):2024-2021.

Sano R., Reed J. C. (2013). ER stress-induced cell death mechanisms. *Biochimica et Biophysica Acta*. **1833**:3460-3470.

Schroder M., Kaufman R. J. (2005). The Mammalian Unfolded Protein Response. *Annual Review of Biochemistry*. **74**:739-789.

Schwartz J. (1991). Particulate air pollution and daily mortality in Detroit. *Environmental Research*. **56**(2):204-213.

Schwartz J., Dockery D. W. (1992). Increased Mortality in Philadelphia Associated with Daily Air Pollution Concentrates. *American Review of Respiratory Disease*. **145**(3): 600-604.

Schwartz J., Marcus A. (1990). Mortality and Air Pollution in London A Time Series Analysis. *American Journal of Epidemiology*. **131**:185-194.

Schwela D. (2000). Air Pollution and Health in Urban Areas. *Reviews on Environmental Health*. **15**(1-2):13-42.

Senft D., Ronai Z. A. (2015). UPR, autophagy, and mitochondria crosstalk underlies the ER stress response. *Trends in Biochemical Sciences*. **40**(3):141-148.

Silva P. J. (2004). Chemical Speciation of $PM_{2.5}$ in Cache Valley. In Cache Valley $PM_{2.5}$ Air Quality Symposium, Logan, UT.

Silva P. J., Vawdrey E. L., Corbett M., Erupe M. (2007). Fine particle concentrations and composition during wintertime inversions in Logan, Utah, USA. *Atmospheric Environment*. **41**:5410-5422.

Sivandzade F., Bhalerao A., Cucullo L. (2019). Analysis of the Mitochondrial Membrane Potential Using the Cationic JC-1 Dye as a Sensitive Fluorescent Probe. *Bio-Protocols*. **9**(1):1-13.

Sotty J., Kluza J., De Sousa C., Tardivel M., Antherieu S., Alleman L.-Y. Canivet L., Perdrix E., Loyens A., Marchetti P., Guidice J.-M. Garcon G. (2020). Mitochondrial alterations triggered by repeated exposure to fine ($PM_{2.5-0.18}$) and quasi-ultrafine ($PM_{0.18}$) fractions of ambient particulate matter. *Environment International*. **142**:1-15.

Sovolyova N., Healy S., Samali A., Logue S. E. (2014). Stressed to death – mechanisms of ER stress-induced cell death. *Journal of Biological Chemistry*. **395**(1):1-13.

Steiner S., Bisig C., Petri-Fink A., Rothen-Rutishauser B. (2016). Diesel exhaust: current knowledge of adverse effects and underlying cellular mechanisms. *Archives of Toxicology*. **90**(7):1541-1553.

Szegezdi E., Logue S. E., Gorman A. M., Samali A. (2006). Mediators of endoplasmic reticulum stress-induced apoptosis. *EMBO Reports*. **7**(9): 880-885.

Tan W.C., Qiu D. Liam B.L., Ng T.P., Lee S. H., van Eeden S. F., D'Yachkova Y., Hogg J.C. (2000). The human bone marrow response to acute air pollution caused by forest fires. *American Journal of Respiratory and Critical Care Medicine*. **161**:1213-1217.

The Salt Lake Tribune, 2004. Logan Air is Dirtiest in the U.S. Friday, 16 January, 2004.

Turner M. C., Drewski D., Diver W. R., Pope III C. A., Burnett R. T., Jerrett M., Marshall J. D., Gapstur S. M. (2017). Ambient Air Pollution and Cancer Mortality in the Cancer Prevention Study II. *Environmental Health Perspectives*. **125**(8):1-10.

U.S. Agriculture Census (2017). Retrieved from https://www.nass.usda.gov/Publications/AgCensus/2017/Online_Resources/County_Profiles/Utah/cp49005.pdf

U.S. Census (2019). Cache County, Utah Population Estimates. Retrieved from https://www.census.gov/quickfacts/fact/table/cachecountyutah,UT/PST045219

USDA (2019). Retrieved from http://furcommission.com/wp-content/uploads/2020/01/mink0719.pdf

Utah State Tax Commission (2020). Retrieved from https://tax.utah.gov/econstats/mv/registrations

USA-Today (2005). Northern Utah residents choke on bad air. USA Today.

Vannuvel K., Renard P., Raes M., Arnould T. (2013). Functional and Morphological Impact of ER Stress on Mitochondria. *Journal of Cellular Physiology*. **228**:1802-1818.

Vattanasit U., Navasumrit P., Khadka M. B., Kanitwithayanun J., Promvijit J., Autrup H., Ruchirawat M. (2014). Oxidative DNA damage and inflammatory responses in cultured human cells and in humans exposed to traffic-related particles. *International Journal of Hygiene and Environmental Health*. **217**(1):23-33.

Vawda S., Mansour R., Takeda A., Funnell P., Kerry S., Mudway I., Jamaludin J., Shaheen S., Griffiths C., Walton R. (2014). *American Journal of Epidemiology.* **179**(4):432-444.

Velali K., Papachristou E., Pantazaki a., Choli-Papadopoulou T., Argyrou N., Tsourouktsoglou T., Lialiaris S., Constantinidis A., Lykidis D., Lialiaris T. S., Besis A., Voutsa D., Samara C. (2016). Cytotoxicity and genotoxicity induced in vitro by solvent-extractable organic matter of size-segregated urban particulate matter. *Environmental Pollution.* **218**:1350-1362.

Walter P., Ron D. (2011). The unfolded protein response: from stress pathway to homeostatic regulation. *Science*. **334**(6059):1081-1086.

Wang D. (2008). Discrepancy between mRNA and protein abundance: Insight from information retrieval process in computers. *Computational Biology and Chemistry*. **32**(6):462-468.

Wang J., Huang J., Wang L., Chen C., Yang D., Jin M., Bai C., Song Y. (2017). Urban particulate matter trigger lung inflammation via the ROS-MAPK-NF-kB signaling pathway. *Journal of Thoracic Disease*. **9**(11):4398-4412.

Wang S., Kaufman R. J. (2012). The impact of the unfolded protein response on human disease. *The Journal of Cell Biology*. **197**(7):857-867.

Wang S., Gillies R. R., Martin R., Davies R. E., Booth M. R. (2012). Connecting Subseasonal Movements of the Winter Mean Ridge in Western North America to Inversion Climatology in Cache Valley, Utah. *Journal of Applied Meteorology and Climatology*. **51**:617-627.

Wang S., Hipps L. E., Chung O., Gillies R. R., Martin R. (2015). Long-Term Winter Inversion Properties in a Mountain Valley of the Western United States and Implications on Air Quality. *Journal of Applied Meteorology and Climatology*. **54**:2339-2352.

Wang Y., Zhong Y., Liao J., Wang G. (2021). $PM_{2.5}$-related cell death patterns. *International Journal of Medical Sciences*. **18**(4):1024-1029.

Watterson T. L., Sorensen J., Martin R., Coulombe Jr. R. A. (2007). Effects of $PM_{2.5}$ Collected from Cache Valley Utah on Genes Associated with the Inflammatory Response in Human Lung Cells. *Journal of Toxicology and Environmental Health*. **70**:1731-1744.

Watterson T. L., Hamilton B., Martin R. S., Coulombe Jr. R. A. (2009). Urban particulate matter causes ER stress and the unfolded protein response in human lung cells. *Toxicological Sciences*. **112**(1):111-122.

Watterson T. L. Hamilton B., Martin R. S., Coulombe Jr. R. A. (2012). Urban particulate matter activates Akt in human lung cells. *Organ Toxicity and Mechanisms*. **86**:121-135.

White A. J., Keller J. P., Zhao S., Carroll R., Kaufman J. D., Sandler D. P. (2019). Air Pollution, Clustering of Particulate Matter Components, and Breast Cancer in the Sister Study: A U.S. -Wide Cohort. *Environmental Health Perspectives*. **127**(10):1-9.

Winterbourn C. (1995). Toxicity of iron and hydrogen peroxide: the Fenton reaction. *Toxicology Letters*. **82-83**(C):969-974.

World Health Organization (2016). Mortality and burden of disease from ambient air pollution. Retrieved from www.who.int/gho/phe/outdoor_air_pollution/burden/en/.

Woodruff T. J., Grillo J., Schoendorf K. C. (1997). The relationship between selected causes of postneonatal infant mortality and particulate air pollution in the United States. *Environmental Health Perspectives*. **105**(6):608-612.

Xia C., Meng Q., Liu L-Z., Rojanaskul Y., Wang X-R., Jiang B-H. (2007). Reactive oxygen species regulate angiogenesis and tumor growth through vascular endothelial growth factor. *Cancer Research*. **67**(22): 10823-30.

Xu X., Jiang S. Y., Wang T-Y., Bai Y., Zhong M., Wang A., Lippmann M., Chen L-C., Rajagopalan S., Sun Q. (2013). Inflammatory Response to Fine Particulate Air Pollution Exposure: Neutrophil verses Monocyte. *PLOS One*. **8**(8):1-8.

Xu X., Qimuge A., Wang H., Xing C., Gu Y., Liu S., Xu H., Hu M., Song L. (2017). IRE1α/XBP1s branch of UPR links HIF1α activation to mediate ANGII- dependent endothelial dysfunction under particulate matter $PM_{2.5}$ exposure. *Scientific Exposure*. **7**(1):1-16.

Yang Y., Liu L., Naik I., Braunstein Z., Zhong J., Ren B. (2017). Transcription Factor C/eBP Homologous Protein in Health and Diseases. *Frontiers in Immunology*. **8**(1612):1-18.

Zhao H., Tong G., Liu J., Wang J., Zhang H., Bai J., Hou L., Zhang Z. (2019). IP3R and RyR channels are involved in traffic-related $PM_{2.5}$-induced disorders of calcium homeostasis. *Toxicology and Industrial Health*. **35**(5):339-348.

Zhou W., Tian D., He J., Zhang Li., Tang X., Zhang L., Wang Y., Li L., Zhao J., Yuan X., Peng S. (2017). Exposure scenario: Another important factor determining the toxic effects of $PM_{2.5}$ and possible mechanisms involved. *Environmental Pollution*. **226**:412-425.

Zhou W., Yuan Z., Zhang L., Su B., Tian D., Li Y., Zhao J., Wang Y., Peng S. (2017). Overexpression of HO-1 assisted $PM_{2.5}$-induced apoptosis failure and autophagy-related cell necrosis. *Ecotoxicology and Environmental Safety*. **145**:605-614.